ELSEVIER

www.elsevier.nl/locate/jorganchem

Journal of Organometallic Chemistry 614–615 (2000) 168–187

Journal of Organometallic Chemistry

Hydridoborates and hydridoborato metallates Part 26. Preparation and structures of dihydridoborates of lithium and potassium

Jörg Knizek, Heinrich Nöth *

Department of Chemistry, Inorganic Chemistry, University of Munich, Butenandtstrasse 5-13, Haus D, D-81377 Munich, Germany

Received 10 April 2000; received in revised form 9 May 2000

Dedicated to Professor Dr S.G. Shore, a great chemist and a very good friend, on the occasion of his 70th birthday.

Abstract

A series of alkali metal dihydrido borates has been prepared by three different routes. They were characterized by ^{11}B-NMR spectroscopy and, in part, by IR spectroscopy. The following compounds were obtained: lithium dihydrido dimethyl borate and lithium methyl trihydrido borate, **1** and **2**, lithium and potassium dihydrido di-*tert*-butyl borate, **3** and **4**, lithium dihydrido dicyclopentyl borate, **5**, lithium and potassium dihydrido 9-borata-bicyclo[3.3.0] nonane, **6a**,**b**, potassium dihydrido boratacyclohexane, **7**, lithium dihydrido boratacycloheptane, **8**, and lithium dihydrido-9-boratafluorene, **9**. In the process of the formation of **1** and **7** also $Li(H_3BMe)$ **2** and $Li_2(H_3B–(CH_2)_5–BH_3)$ are formed, most likely by a ligand redistribution process which is not operative if bulky organyl groups are bound to the boron atom or if the boron atom is part of a ring system. In case of catecholate no $H_2B(OR)_2^-$ anions were detected but for ephedrino or dithiolato ligands the corresponding dihydrido borate complexes were readily detected by ^{11}B-NMR but the latter converted in THF solution into $B(S_2R')_2$ anions. MO calculations show that the ligand redistribution for $H_2BX_2^-$ ions into BH_4^- and BX_4^- becomes thermodynamically more favored with increasing electronegativity of the substituent X. Characterization of the new hydrido borate species is usually unambiguous, but **10** shows an anomalous temperature dependent behavior in THF solution which can be attributed to an equilibrium involving Li(2H, 2O), Li(2H, 3O), and Li(3O) structural units. This is supported by the X-ray structure of dimeric **10**·THF and monomeric **10**·THF·TMEDA. While **9**·3THF is monomeric and contains doubly bridging H_2B groups all other dihydrido diorganyl borates are dinuclear. The interaction between the alkali metal center and the boron bonded H atoms depends on number and size of the auxiliary ligands. 'Agostic' Li···H–C interactions play a role if β-H atoms are present and when the alkali metal cation is not coordinatively saturated by the auxiliary ligand and the H(B) hydrogens. The most symmetric and so far unique arrangement is found for $[\mathbf{6a}\cdot 2THF]_2$ where all four H(B) hydrogens form Li···H···Li bridges. Also lithium bis(dithiocatecholato)borate, **17**·2 THF is dimeric. Its Li centers are coordinated by four sulfur and two oxygen atoms. These atoms form a double heterocubane structure with two diametral edges missing. © 2000 Elsevier Science B.V. All rights reserved.

Keywords: Hydridoborates and hydridoborato metallates; Dihydridoborates; Lithium; Potassium

1. Introduction

The tetrahydridoborate group BH_4^- is a versatile ligand showing a large variation of metal–hydrogen interactions with alkali metal cations [2–7]. The size of the cation, the denticity of the auxiliary ligand coordinating to the alkali metal cation and its steric requirements determine the topology of the interaction with the BH_4^- anion. Structures in the solid state range from mononuclear, molecular species (or contact ion pairs) to three dimensional arrays. Replacement of the hydrogen atoms at the boron center by organyl groups should result in a more or less drastic modification of the M···H–B interaction. A typical example is $Na[HBMe_3]\cdot OEt_2$, **1**, which is tetrameric with a cube shaped Na_4H_4 structural moiety [8]. So far no systematic structural study has been reported regarding the

* Corresponding author. Fax: +49-89-21807455.
E-mail address: h.noeth@lrz.uni-muenchen.de (H. Nöth).

0022-328X/00/$ - see front matter © 2000 Elsevier Science B.V. All rights reserved.
PII: S0022-328X(00)00688-4

influence of substituents at the boron atom of a dihydridoborate unit on the interaction with alkali metal cations. As far as we are aware there exists also no structural information on monosubstituted complexes of type $M[H_3BR]$. However, the structures of a series of alkali metal aminotrihydridoborates $M[R_2NBH_3]\cdot nL$ are now well documented. These compounds are characterized not only by M···H–B interactions but also by M–N bonds. [3] Most of the dihydrido diorganyl borates of the alkali metals have only been investigated by NMR methods [1–18], but the degree of association of these hydridoborates in solution is almost unknown, and may be different to the solid state structure. Unfortunately, ^{11}B-NMR data give no information as to the interaction between the alkali metal cation and the organylhydridoborate anion. Moreover, the IR spectra are in many cases also not very informative.

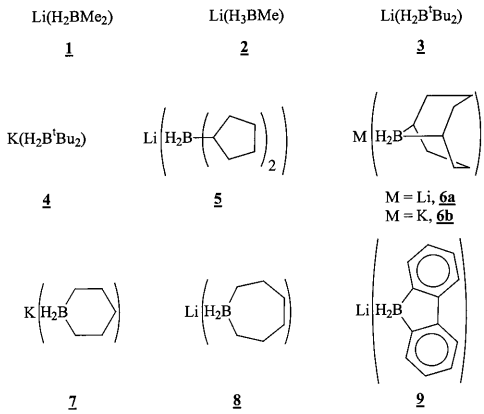

2. Preparation

From the numerous known methods to prepare substituted hydridoborates we applied those summarized in Eqs. (1)–(3).

$$HBR_2 + MH \rightarrow M(H_2BR_2) \quad (1)$$

$$HalBR_2 + 2MH \rightarrow M(H_2BR_2) + MHal \quad (2)$$

$$MBH_4 + 2(RX)H \rightarrow M(H_2B(XR)_2) + 2H_2 \quad (3)$$

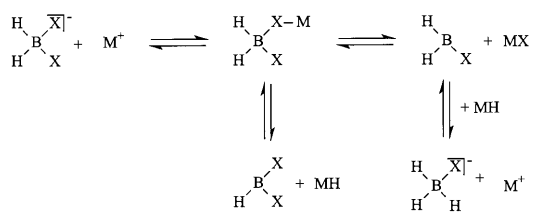

(4)

$$2LiBH_2(SR'S) \rightarrow LiBH_4 + LiB(SR'S)_2 \quad (5)$$

The reaction according to Eq. (1) was successfully applied for the dihydrido-diorganyl-borates **1**, **2**, **9** and **10**, while method (2) was used for obtaining **5**, the potassium salt of the dihydrido-9-borata-[3.3.0]bicyclononane anion, **6**, as well as **8**. Finally, the reaction as depicted in Eq. (3) was employed for obtaining compounds **12**–**15**. Polar solvents are required to induce rapid reactions. In most cases good yields — as determined by ^{11}B-NMR spectroscopy — were obtained. However, yields were low or even negligible if the dihydrido diorganyl borate had a high tendency to undergo substituent exchange as shown in Eq. (4). Thus, a solution of $Li(H_2BMe_2)$ in THF on standing led to crystalline $Li[H_3BMe]\cdot 2THF$, **2**·2THF. This organyl group exchange is preferentially observed for noncyclic H_2BR_2 anions but not, for instance, for $Li[H_2Bfl]$ (Bfl = 9-borafluorenyl), **9**, or $K[H_2$-9-BBN] (9-BBN = 9-borata[3.3.0]bicyclononyl), **6b**.

This ligand exchange is particularly pronounced in the case of alkoxo and thiolato ligands. Several futile attempts have been reported for the synthesis of lithium dihydridocatecholato borate **11** by reacting catecholborane with LiH, $NaHBEt_3$ or $NaBH_4$ [19,20]. Only **16** besides MBH_4 was obtained. The same behavior was now observed by reacting monolithium catecholate with BH_3THF (1:1) in THF–hexane at 0°C. The ^{11}B-NMR signal at -40.8 ppm (quintet) and 11.9 ppm (singlet) showed the formation of $LiBH_4$ and $LiB(O_2C_6H_4)_2$ [21] in a 1:1 ratio. In addition, a broad low intensity signal centered at 9 ppm ($h_{1/2} = 180$ Hz) whose multiplicity could not be resolved, points to the formation of a third species, but no definite assignment can be made for this signal.

The potassium dihydrido[4S,5R]ephedrino borate **13** was detected in THF solution by reacting the corresponding oxazaborolidine **19**, prepared from ephedrine and $BH_3\cdot$THF in THF with KH in the presence of 18-crown-6. The resulting solution showed three ^{11}B-NMR signals at $\delta = 4.6$ (triplet, $^1J(^{11}B^1H) = 90$ Hz), -10.7 ($h_{1/2} = 380$ Hz) and 10.6 ppm, the ratio being 22:39:39. The signal at -10.9 ppm is due to compound **13**, the other two signals can be assigned to the anomalous structure of the oxazaborolidine **20**. Thus, **19** dimerizes by KH to give **20** and only a part of **19** is converted into **13**.

The reaction of $LiBH_4$ with benzene-1,2-dithiol lead to the formation of benzene-1,2-dithiolato dihydrido borate **14** as described by Eq. (5). The solution also contains the spirocyclic lithium bis(benzene-1,2-dithiolato)borate **17**. **14** changes into $LiBH_4$ and **17**, the latter crystallizes from the THF solution as **17**·2 THF. By using ethanedithiol the same behavior is observed. Thus, the anion $H_2B(S_2C_2H_4)^-$, **15**, was readily detected by ^{11}B-NMR spectroscopy but ligand exchange to $LiBH_4$ and **18** occurs also.

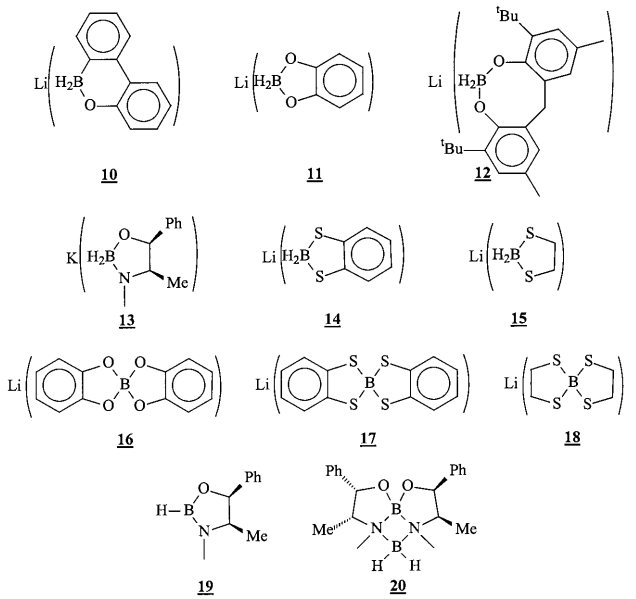

Table 1
^{11}B chemical shifts (in ppm) and $^{1}J(^{1}H^{11}B)$ coupling constants (Hz) of alkali metal hydridoborates

	$\delta^{11}B$ (ppm)	$^{1}J(^{11}B^{1}H)$ (Hz)	Solvent
LiH_3Bme	−31.6	74	THF–pentane
$Li(H_2Bme_2)$	−23.9	70	THF–pentane
$Li(H_3B(CH_2)_6BH_3)$	−26.1	75	THF
$LiH_2B(CH_2)_6$	−16.4	71	THF
$LiH_2BC_8H_{14}$	−16.6	71	C_6D_6
$LiH_2B(C_5H_9)_2$	−14.1	68	THF
$LiH_3BC_5H_9$	−25.9	75	THF
$KH_2B(CMe_3)_2$	−2.8	71	C_6D_6
LiH_2Bfl	−22.3	78	$CDCl_3$
$LiH_2BOC_{12}H_8$	−3.9	See text	THF
$LiH_2BO_2C_6H_4$	9.0* (?)		THF–hexane (* broad)
$KH_2BONC_{10}H_{13}$	4.6	90	THF
$LiH_2BS_2C_6H_4$	−11.0	110	THF
$LiH_2BS_2C_2H_4$	−13.2	111	THF

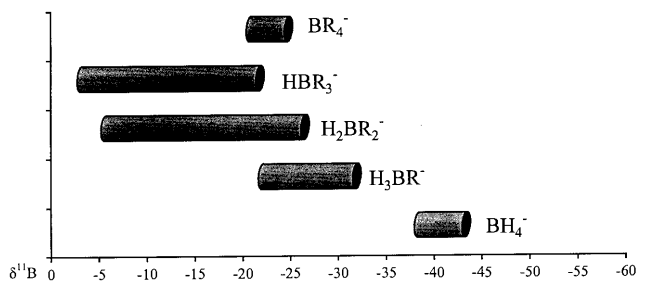

Fig. 1. ^{11}B chemical shift ranges for organylhydridoborates BR_nH_{4-n}.

3. ^{11}B-NMR and IR data

The new hydridoborates of the alkali metals are soluble in diethylether, tetrahydrofuran, and some of them even in hydrocarbon solvents such as hexane or toluene. Their ^{11}B chemical shifts are presented in Table 1 together with the coupling constants $^{1}J(^{11}B^{1}H)$. These new data together with other data for hydrido organyl borates reported in the literature are presented as an overview on the $\delta^{11}B$ ranges for their alkali metal compounds in Fig. 1.

Obviously these ranges are fairly characteristic for the degree of alkyl substitution. Assignment is of course readily made by the coupling patterns although for monohydrido triorganyl borates only a broad signal and not a doublet may be observed [16,22] particularly in hydrocarbon solvents. Alkylation of the BH_4^- ion results in a deshielding of the boron nuclei whereas these are better shielded in tetraalkylborate ions than in hydridotrialkyl borate ions. The method of additive parameters does not reproduce the experimental data sufficiently well. This suggests that the solution state of the individual hydrido organyl borates may have different degrees of association. However, it should be noted that a triplet at $\delta^{11}B = -2.8$ for $K[H_2B(t\text{-}Bu)_2]$, **4**, observed for a benzene solution of the non solvated compound, shows an unusually deshielded boron nucleus while the coupling constant $^{1}J(^{11}B^{1}H) = 71$ Hz has the expected value. The same is true for lithium or potassium dihydridodiisopinocamphylborate [13,14]. This may result from a steric effect because the cation has only a marginal effect if any on $\delta^{11}B$ in these compounds. [13,14] The rather unusual shielding of the ^{11}B nucleus of **4** may be due to the steric repulsion of the two *tert*-butyl groups. Indeed, an increase in the steric demand of the alkyl substituent can be noted by inspecting the $\delta^{11}B$ values of $Li(H_2BMe_2)$ (-21.8 ppm), LiH_2BEt_2 (-14.2 ppm) and $LiH_2Bi\text{Pr}_2$ (-7.6 ppm) [16].

In order to evaluate the influence of the C–B–C bond angle on $\delta^{11}B$ the hypersurface for the $^{t}Bu_2BH_2^-$ anion was investigatd for the anion $Me_2BH_2^-$ as a model by ab initio calculations. Under the condition that the B–C bond length remains constant at the local minimum (1.619 Å) the C–B–C bond angle has been changed from 90 to 140° in 5° increments. At these points the screening constant for the boron nucleus was calculated using the GIAO method on the HF/6-311-G(d) level [29]. The data have been normalized for B_2H_6 ($\delta^{11}B = 16.6$ ppm). Fig. 2 shows the influence of the variation of the bond angle on $\delta^{11}B$. Within the 95–110° limit there is almost no change in $\delta^{11}B$ and the shielding is at a minimum. The values of the chemical shifts are quite different from that of the $H_2Bt\text{Bu}_2$ anion, nevertheless the wide bond angle of the di-*tert*-butylborate has some resemblance with the calculated values for the model anion $Me_2BH_2^-$.

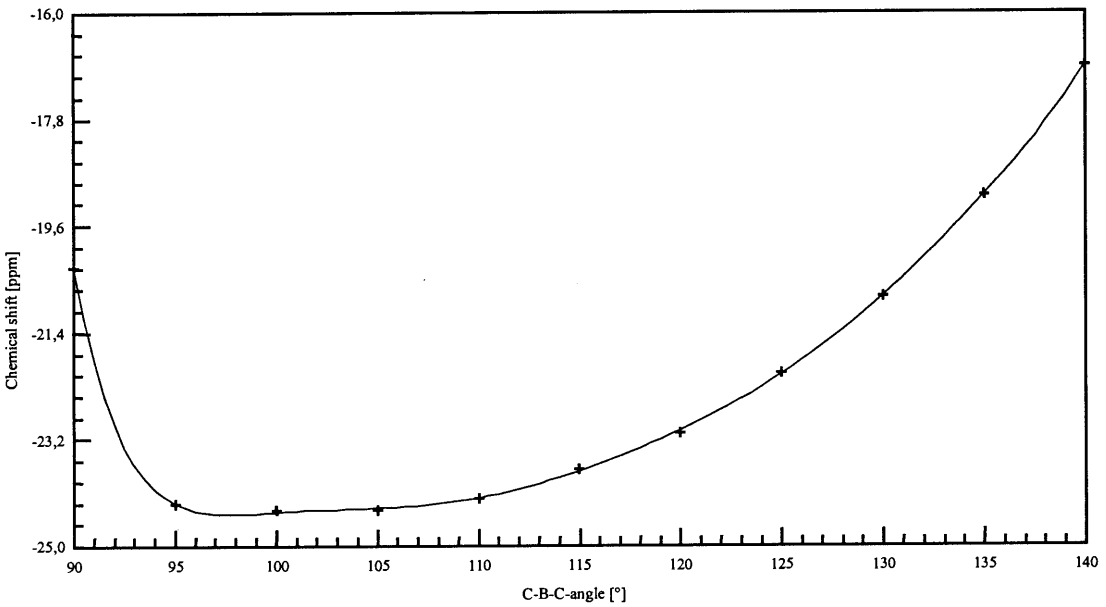

Fig. 2. Dependence of the C–B–C bond angle on δ^{11}B for the anion $Me_2HB_2^-$.

Compound **10** is the first stable oxosubstituted dihydridoborate. Its ^{11}B-NMR spectrum shows a broad, unresolved signal at $\delta = -3.9$ at ambient temperature. On heating the solution to 40°C the signal becomes sharp enough to reveal a triplet with $^1J(^{11}B^1H) = 91$ Hz as expected for a dihydrido borate (see Fig. 3). Its chemical shift remains independent of temperature. A possible explanation for this behavior is an equilibrium as shown in Eq. (6)

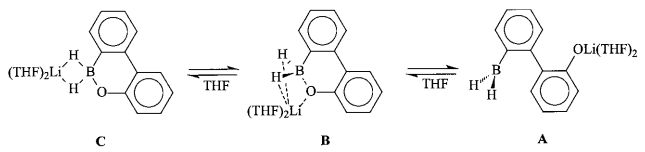

(6)

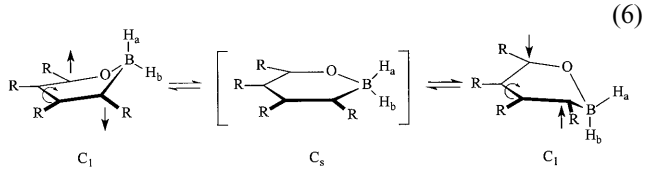

(7)

The presence of a tricoordinated species such as **A** formed by ring opening can be excluded not only by the ^{11}B-NMR data but also by the IR spectrum (in THF solution) because this does not display any BH stretching bands in the region of 2600–2700 cm^{-1}, typical for B–H bonds to tricoordinated boron atoms. Prominent bands are, however, found at 2228, 2247 and 2289 cm^{-1}. The first and last of these bands can be assigned to ν_{asym} and ν_{sym} BH_2 stretching vibrations (Fig. 4(a)). The band at 2247 cm^{-1} results from ν_{asym} $^{10}BH_2$ [23,24]. A completely different IR spectrum results for solid **10** (see Fig. 4(b)). This indicates that the structure of **10** in THF solution and the solid state are quite different.

An alternative explanation for the temperature dependent ^{11}B-NMR spectrum in solution could be a change of ring conformation as described by Eq. (7). Actually, if the ring system is not planar, then the two H–B atoms are not chemically equivalent; two doublets might be observable if the inversion process is slow. At ambient temperature the ^{1}H-NMR spectrum shows only one set of signals for the THF molecules of **10**·2 THF and for the ring system, however, no signals for the B bonded hydrogen atoms could be detected. Therefore, this spectrum is a time averaged NMR spectrum. X-ray structures of **10**·2THF and **10**·THF·TMEDA lends credence to the equilibria shown in Eqs. (6) and (7).

While Table 1 contains the ^{11}B-NMR data of the hydrido borates reported here, Table 2 summarizes chemical shift data and coupling constants for published hydrido borates for purpose of comparison. Organyloxo and organylthio, as well as nitrogen substituted dihydrido borates are also included. The chemical shifts indicate that the shielding is primarily determined by the electron withdrawing effect and the number of the substituents. The boron nucleus of oxygen and nitrogen containing dihydrido borates are less well shielded than the sulfur containing species which approach already the range found for dialkyl dihydrido borates. In addition, the $^1J(^{11}B^1H)$ coupling constants are characteristic for each of the disubstituted dihydrido borates. Since it is well known that the coupling represents the s-orbital contribution to coupling transmission one can assume that the H–B–H bond angles change significantly within these series of compounds.

4. X-ray structure determinations

The structure of solvates of compounds **2**, **4**, **6a**,**b**, **9**, **10** and **17** have been determined by X-ray diffraction methods. Relevant crystallographic data and data referring to data collection and structure refinement are summarized in Table 3.

The crystal structure of $Li(H_2BMe_2)$, **1**, could not be determined because the compound precipitated only as a microcrystalline powder from a THF solution at −30°C. However, $Li(H_3BMe)\cdot 2THF$, **2**·2THF, separated from the solution as single crystals suitable for a structure determination. It crystallizes in the monoclinic system in space group $P2_1/c$. The molecule is present in the lattice as a centrosymmetric dimer as depicted in Fig. 5. The crystallographic inversion center is located at the center of a planar Li_2B_2 four-membered ring. Each Li center is coordinated by four hydrogen atoms and two oxygen atoms. However, although the Li atoms are hexa-coordinated the coordination polyhedron is far from being close to an octahedral array. This is the consequence of the rather acute H···Li···H angles. Each H_3BMe^- group supplies three H atoms to coordinate with the Li centers, one hydrogen atom binds to both Li ions, the other two only to one. Thus the H_3BMe unit is of the type $2\mu_1^1$, μ_1^2, a structural pattern that is well known for dimeric $LiBH_4\cdot$TMEDA [5]. Li–H and B–H distances are within the expected ranges, consequently the Li···B distances (2.507 Å) are larger than the sum of covalent radii (2.4 Å).

In contrast to **2**·2THF the dihydridoborate $Li[H_2Bfl]\cdot 3THF$ (Bfl = 9-borafluorenyl), **9**·3THF, crystallizes as a mononuclear species, and its molecular structure is shown in Fig. 6. Its Li center is penta-coordinated by three oxygen and two hydrogen atoms. One might, therefore, expect either a trigonal bipyramidal or tetragonal pyramidal arrangement of the ligands around the Li ion. However, the rather sharp H···Li···H angle excludes any of these features. Taking the O–Li–O bond angles into account which range from 101.9 to 105.9° these suggest a coordination sphere closer to tetrahedral. This is indeed the case if we consider not the hydrogen atoms but rather the boron

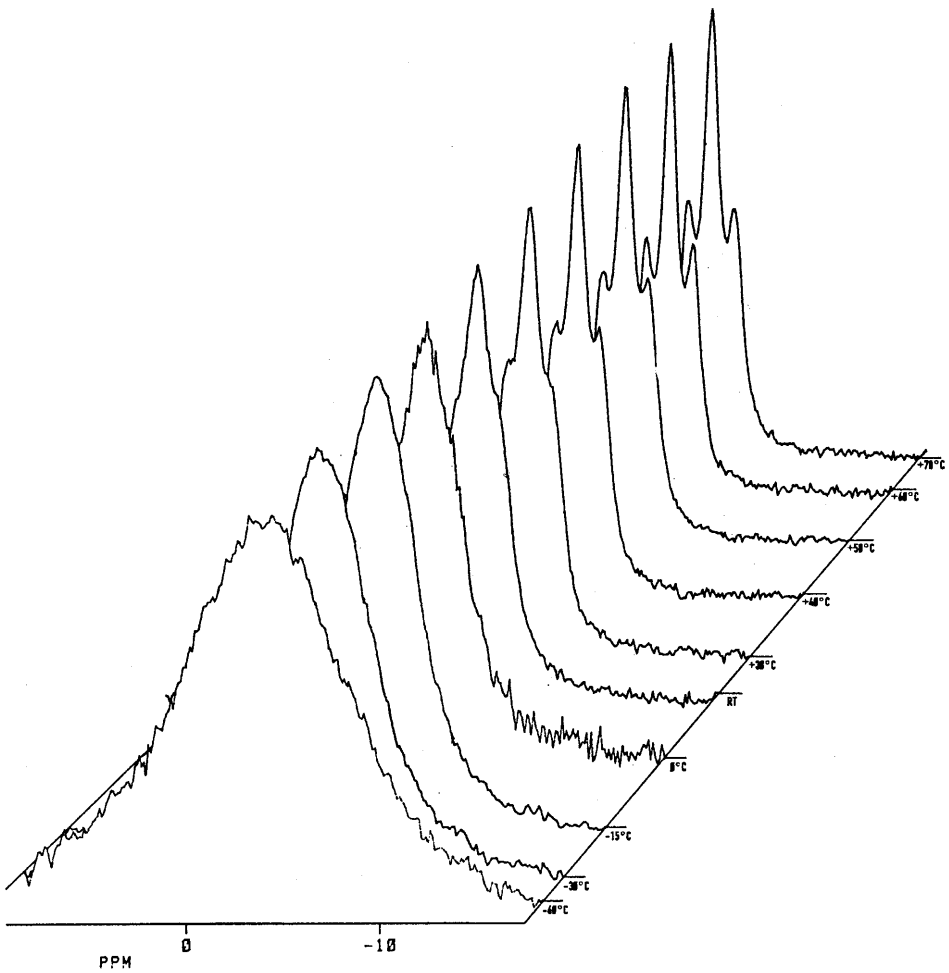

Fig. 3. Temperature dependent ^{11}B-NMR spectrum of **10** in THF solution.

Table 3
Crystallographic data and selected information on data collection and refinement

Compound	**2**	**9** (3THF)	**6a** (OEt_2)	**6a** (2THF)	**6a**·THF·TMEDA	**4**·PMDTA	**12** (THF TMEDA)	**17** (2THF)
Empirical formula	$C_9H_{22}BLiO_2$	$C_{24}H_{34}BLiO_3$	$C_{24}H_{52}B_2Li_2O_3$	$C_{32}H_{64}B_2Li_2O_4$	$C_{26}H_{56}B_2Li_2N_2O$	$C_{17}H_{43}B\,KN_3$	$C_{22}H_{34}BLiN_2O_2$	$C_{20}H_{24}BLiO_2S_4$
Formula weight	180.02	388.26	408.16	548.33	448.23	339.45	376.26	442.38
Crystal size (mm)	$0.10\times0.50\times0.60$	$0.40\times0.50\times0.60$	$0.60\times0.30\times0.30$	$0.2\times0.3\times0.3$	$0.2\times0.2\times0.2$	$0.20\times0.20\times0.30$	$0.20\times0.20\times0.30$	$0.2\times0.3\times0.3$
Crystal system	Monoclinic	Orthorhombic	Monoclinic	Orthorhombic	Monoclinic	Triclinic	Monoclinic	Orthorhombic
Space group	$P2_1/c$	$Pna2_1$	$C2/c$	$P2_12_12_1$	$P2_1/c$	$P1$	$P2_1/n$	$Pbca$
a (Å)	9.6021(6)	12.8540(1)	19.3660(3)	9.903(7)	12.920(5)	9.4418(3)	12.4774(3)	14.335(8)
b (Å)	14.15(1)	19.4650(2)	7.4127(2)	18.34(1)	12.562(4)	11.1407(4)	13.6848(5)	16.942(7)
c (Å)	9.8958(8)	9.2360(2)	19.6464(1)	19.05(1)	18.542(7)	12.3215(4)	13.4866(4)	18.111(8)
α (°)	90	90	90	90	90	87.658(1)	90	90
β (°)	115.159(2)	90	100.220(1)	90	102.86(1)	69.952(1)	100.349(1)	90
γ (°)	90	90	90	90	90	74.014(1)	90	90
V (Å^3)	1217.37(16)	2310.88(6)	2775.58(9)	3458.7(38)	2933.7(19)	1154.98(7)	2265.38(12)	4398.5(36)
Z	4	4	4	4	4	2	4	8
ρ_{calc} (mg m^{-3})	0.982	1.116	0.977	1.053	1.015	0.976	1.103	1.336
μ (mm^{-1})	0.063	0.070	0.056	0.064	0.058	0.232	0.068	0.445
$F(000)$	400	840	912	1216	1000	380	816	1856
Index range	$-10\le h\le12$	$-16\le h\le13$	$-24\le h\le12$	$-12\le h\le12$	$-15\le h\le15$	$-12\le h\le12$	$-12\le h\le14$	$-18\le h\le18$
	$-18\le k\le18$	$-25\le k\le25$	$-9\le k\le7$	$-23\le k\le23$	$-13\le k\le13$	$-13\le k\le13$	$-16\le k\le16$	$-22\le k\le22$
	$-12\le l\le12$	$-11\le l\le11$	$-24\le l\le24$	$-21\le l\le21$	$-21\le l\le21$	$-15\le l\le15$	$-16\le l\le16$	$-20\le l\le21$
2θ (°)	57.38	58.30	56.58	54.80	49.42	58.42	52.02	58.22
Temperature (K)	173(2)	183(2)	183(2)	193	183(2)	183(2)	173(2)	183(2)
Reflections collected	6792	12858	6409	18006	13760	6648	11639	24708
Reflections unique	2343	4606	2683	6751	4660	3633	3443	4750
Reflections observed (4σ)	1410	3409	2072	2821	3092	3124	2587	2742
R_{int}	0.0333	0.0248	0.0420	0.0822	0.1041	0.0133	0.0440	0.0605
Variables	169	319	128 (28 restraints)	378	345	218	265	253
Weighting scheme [a] x/y	0.0838/0.5753	0.0669/0.1369	0.058/2.788	0.1186/2.0106	0.0000/4.6790	0.0583/0.3133	0.0410/1.9825	0.0248/7.4727
Goodness-of-fit	1.053	1.045	1.133	1.111	1.268	1.038	1.063	1.151
Final R (4σ)	0.0732	0.0443	0.0684	0.0841	0.1199	0.0392	0.0681	0.0500
Final wR_2	0.1735	0.1104	0.1610	0.2045	0.1896	0.1040	0.1396	0.0986
Largest res. peak (e Å^{-3})	0.185	0.141	0.1474	0.282	0.246	0.258	0.342	0.316

[a] $w^{-1}=\sigma^2F_o^2+(xP)^2+yP;\ P=(F_o^2+2F_c^2)/3.$

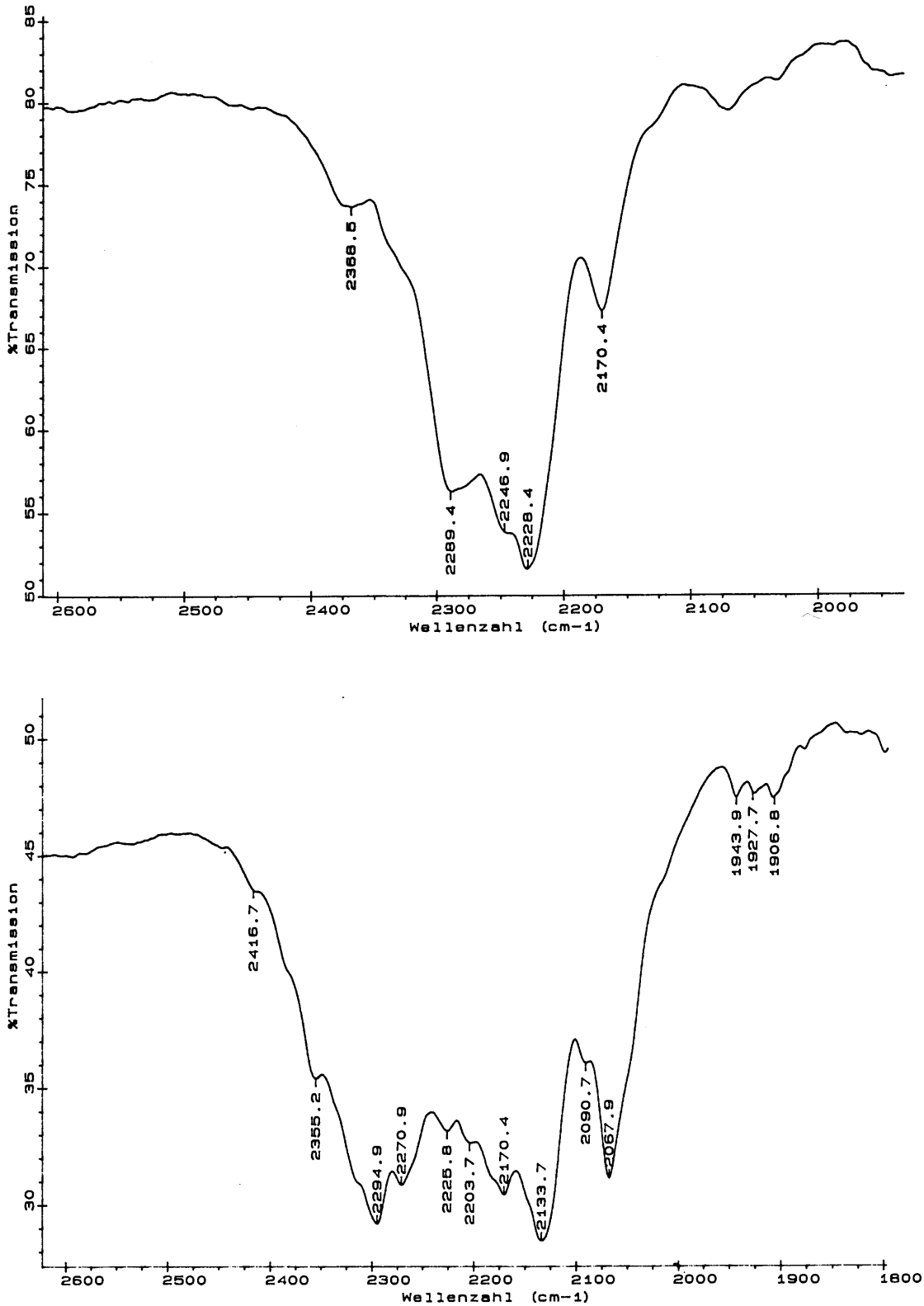

Fig. 4. IR spectra for the νBH region (a) for **10** in THF solution; (b) for **10** as a suspension in Nujol.

atom as a coordination point because the O–Li–B bond angles range from 107.7 to 120.5°. On the other hand, the Li···B distance is 2.454(4) Å, and although this is slightly larger than the sum of covalent radii it approaches a non negligible interaction between the two atoms.

Table 2
^{11}B chemical shifts (in ppm) and $^{1}J(^{1}H^{11}B)$ coupling constants (Hz) published for hydrido organyl borates [a]

	$\delta^{11}B$ ($^{1}J_{BH,}$ solvent)	Literature
Na $H_2B(CN)_2$	−36.35 (t, 92.8 Hz, Me_2SO-d_6)	[11]
n-Bu_4 $H_2B(CN)_2$	−41.44 (t, 92.8 Hz, $CDCl_3$)	[11]
1	−4.9 (d, 70 Hz, THF-d_8)	[12]
2	6.7 (s, CH_2Cl_2)	[12]
3	−10.4 (s, CH_2Cl_2)	[12]
4	−13.7 (d, 70 Hz, (CH_2Cl_2)	[12]
Li H_2BBN	−17.4 (t, 74 Hz, THF)	[13]
Na H_2BBN	−18.3 (t, 74 Hz, THF)	[13]
K H_2BBN	−16.3 (t, 74 Hz, THF)	[13]
Li H_2BBN	−17.4 (t, 72.1 Hz, THF)	[14]
Li disiamylborate	−14.8 (t, 69.0 Hz, THF)	[14]
Li thexylborate	−24.47 (q, 71.0 Hz, THF)	[14]
Na H_2BBN	−18.37 (t, 72.0 Hz, THF)	[14]
Na disiamylborate	−14.95 (t, 71.0 Hz, THF)	[14]
Na dicyclohexyl-borate	−11.82 (t, 71.8 Hz, THF)	[14]
Na thexylborate	−25.69 (q, 72.0 Hz, THF)	[14]
K H_2BBN	−16.27 (t, 69.0 Hz, THF)	[14]
K disiamylborate	−13.06 (t, 71.0 Hz, THF)	[14]
K diisopino-camphylborate	−4.84 (t, 69.0 Hz, THF)	[14]
K thexylborate	−21.74 (q, 71Hz, THF)	[14]
K monoisopino-camphylborate	−21.20 (q, 71.0 Hz, THF)	[14]
Li H_2BBN	−14.15 (t, 69 Hz, THF)	[15]
Li dicyclohexyl-borate	−9.28 (t, 67 Hz, THF)	[15]
Li disiamylborate	−12.21 (t, 67 Hz, THF)	[15]
Li diisopino-camphylborate	−5.69 (t, 68 Hz), THF)	[15]
Li cyclopentylborate	−26.6 (q, 74 Hz, THF)	[15]
Li cyclohexylborate	−25.4 (q, 74 Hz, THF)	[15]
Li norbornylborate	−25.7 (q, 75 Hz, THF)	[15]
Li siamylborate	−27.5 (q, 75 Hz, THF)	[15]
Li isopino-camphylborate	−23.5 (q, 76 Hz, THF)	[15]
Li thexylborate	−24.4 (q, 77 Hz, THF)	[15]
Li Me_2BH_2	−21.80 (t, 64 Hz, Et_2O)	[16]
Li Et_2BH_2	−14.20 (t, 67 Hz, Et_2O)	[16]
Li *n*-Pr_2BH_2	−11.53 (t, 67 Hz, Et_2O)	[16]
Li *i*-Pr_2BH_2	−7.59 (t, 62 Hz, Et_2O)	[16]
Li *n*-Bu_2BH_2	−16.07 (t, 61 Hz, Et_2O)	[16]
Li *sec*-Bu_2BH_2	−9.62 (t, 68 Hz, Et_2O)	[16]
Li *i*-Bu_2BH_2	−19.09 (t, 67 Hz, Et_2O)	[16]
Li cyclopentyl$_2BH_2$	−11.24 (t, 68 Hz, Et_2O)	[16]
Li cycloheptyl$_2BH_2$	−13.83 (t, 67 Hz, Et_2O)	[16]
Li cyclooctyl$_2BH_2$	−14.70 (t, 68 Hz, Et_2O)	[16]
Li benzyl$_2BH_2$	−12.88 (t, 72 Hz, Et_2O)	[16]
Li $MeBH_3$	−31.4 (q, 70.3 Hz, Hexan/THF)	[17]
Li *n*-$BuBH_3$	−29.0 (q, 74 Hz, Hexane/THF)	[17]
Li *sec*-$BuBH_3$	−25.3 (q, 77 Hz, Hexane/THF)	[17]
Li $Me_3SiCH_2BH_3$	−31.7 (q, 78 Hz, Hexane/THF)	[17]
Li *t*-$BuBH_3$	−21.2 (q, 77.7 Hz, Hexane/THF)	[17]
Li Me_2BH_2	−23.6 (t, 66.6 Hz, Hexane/THF)	[17]
Li *n*-Bu_2BH_2	−19.2 (t, 70 Hz, Hexane/THF)	[17]
Li *sec*-Bu_2BH_2	−11.9 (t, 74 Hz, Hexane/THF)	[17]
Li *t*-Bu_2BH_2	−6.4 (t, 70.3 Hz, Hexane/THF)	[17]
Li Me_3BH	−21.0 (d, 66.6 Hz, Hexane/THF)	[17]
Li *n*-Bu_3BH	−14.4 (d, 75 Hz, Hexane/THF)	[17]
Li *sec*-Bu_3BH	−6.7 (d, 73 Hz, Hexane/THF)	[17]
Li *t*-Bu_3BH	−2.3 (d, 83 Hz, Hexane/THF)	[17]
Li Me_4B	−20.7 (Hexane/THF))	[17]
Li (*n*-Bu)$_4$B	−17.5 (Hexane/THF)	[17]
Li *n*-Bu_2BH_2	−16.4 (t, 67 Hz, THF)	[18]
Li *n*-Hex_2BH_2	−16.4 (t, 67 Hz, THF)	[18]
Li (2-methyl-1-propyl)$_2BH_2$	−19.1 (t, 67 Hz, THF)	[18]

Table 2 (*Continued*)

	δ^{11}B ($^1J_{BH}$, solvent)	Literature
Li (3-methyl-2-butyl)$_2$BH$_2$	−12.3 (t, 68 Hz, THF)	[18]
Li cyclohexyl$_2$BH$_2$	−9.3 (t, 67 Hz, THF)	[18]
Li $(CH_2)_4BH_2$	−20.2 (t, 71 Hz, THF)	[18]
Li $(CH_2)_5BH_2$	−18.9 (t, 68 Hz, THF)	[18]
$(CH_2)_5B(NH_3)_2^+$ $(CH_2)_5BH_2^-$	(−5.95, s) −19.50 (t, 73 Hz,)	[19]
Na $(CH_2)_5BH_2$	−22.13 (t, 72 Hz, THF)	[19]

a

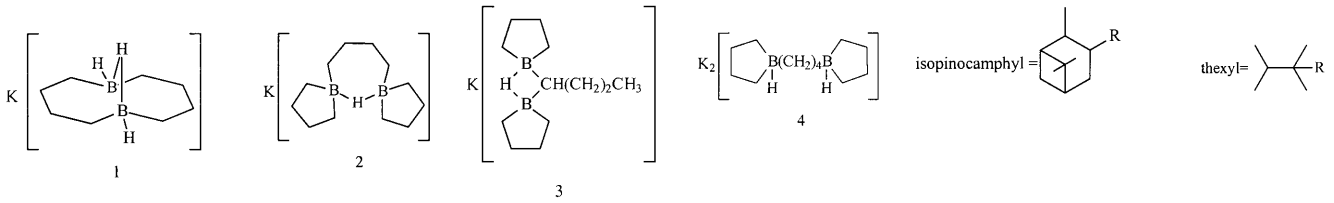

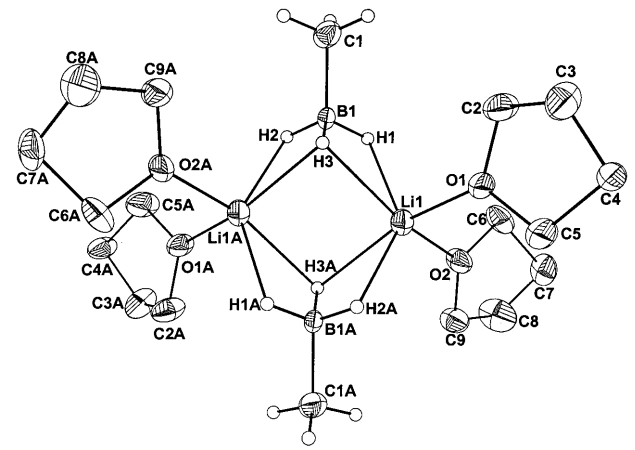

Fig. 5. The molecular structure of dimeric lithium methyltrihydrido borate 2-tetrahydrofuran, **2·2THF**, in the crystal. Thermal ellipsoides are depicted on a 25% probability level. Selected atom distances (Å): Li1–H1 2.01(2), Li1–H2A 2.00(2), Li1–H3 2.13(2), Li1–H3A 2.11(2), Li1–O1 1.956(4), Li1–O2 1.971(4), B1–H1 1.02(2), B1–H2 1.01(2), B1–H3 1.10(3), B1–C1 1.597(4), Li1···B1 2.507(2), Li1···B1A 2.497(2). Selected bond angles (°): B1–Li1–B1A 103.9(2), O1–Li1–O2 98.8(2), B1–Li1–O1 104.5(2), B1–Li1–O2 122.9(2), B1A–Li1–O1 124.6(2), B1A–Li1–O2 104.1(2), H1–B1–H2 105(2), H1–B1–H3 108(2), H2–B1–H3 106(2), C1–B1–H1 114(1), C1–B1–H2 113(1), C1–B1–H3 112(1), Li1A–H3–Li1 93.5(9), Li1–H1–B1 107(2), Li1A–H2–B1 108(2). Atoms C3 and C4 are disordered by a twist through the center of the C3–C4 bond. The configuration with SOF 59% is depicted.

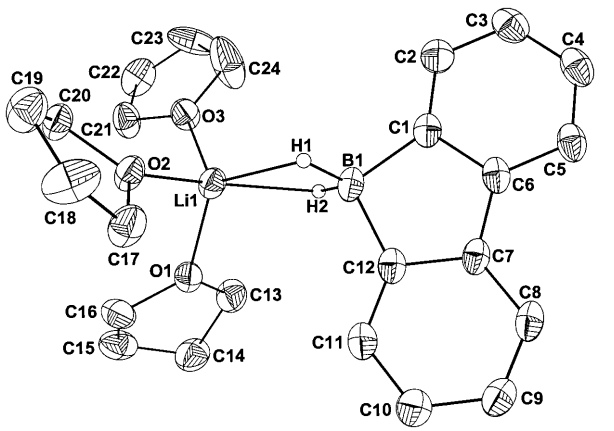

Fig. 6. The molecular structure of **9·3THF**, in the crystal. Thermal ellipsoids represent a 25% probability. Selected atom distances (Å): Li1–O1 1.948(4), Li1–O2 1.956(4), Li1–O3 1.923(4), Li1–H1 1.98(2), Li1–H2 2.01(2), B1–C1 1.624(3), B1–C12 1.610(3), C1–C6 1.410(3), C6–C7 1.469(3), C7–C12 1.411(3), B1–H1 1.16(2), B1–H2 1.17(2). Selected bond angles (°): O1–Li1–O2 101.9(2), O1–Li1–O3 105.9(2), O2–Li1–O3 104.3(2), B1–Li1–O1 107.7(2), B1–Li1–O2 120.5(2), B1–Li1–O3A 115.0(2) H1–Li1–H2 55.2(9), H1–B1–H2 106(2), C1–B1–C12 99.8(2), H1–B1–C1 115(1), H1–B1–C12 114(1), H2–B1–C1 112(1), H2–B1–C12 111(1). Interplanar angle: H1Li1H2–H1B1H2 = 16°.

An unexpected feature of the structure of **9**·3THF is the bending of the H_2B unit with respect to the LiH_2 plane by 16°. This bending is most likely due to packing effects because the interaction between the solvated Li cation and the H_2Bfl anion is primarily determined by electrostatic forces.

As expected, the 9-borafluorene unit is practically planar, the largest deviation from the mean plane being only 0.04 Å. Its B–C bonds (average 1.617 Å) are longer than the B–C bond in compound **2**·2THF (1.597 Å) but shorter than the B–C bonds in **4**·PMDTA (1.642, 1.644 Å).

Three solvates of lithium dihydrido boratabicyclo[3.3.0]nonane **6** could be isolated as single crystals: dimeric **6a**·OEt_2, dimeric **6a**·2THF, and (**6a**)$_2$·THF·TMEDA. All three compounds are characterized by dimeric **6a** units in the solid state.

Fig. 7 shows the molecular structure of **6a**·OEt_2 There is a crystallographic C_2 axis which generates the

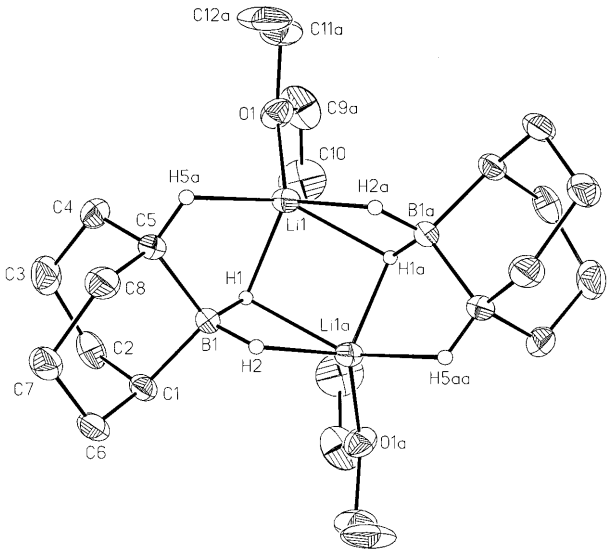

Fig. 7. Structure of lithium 9-borata-bicyclo[3.3.0]nonane, **6a**·Et_2O, in the crystal. Thermal ellipsoides are depicted at 25% probability. Selected atom distances (Å): Li1–O1 1.904(4), Li1···B1 2.392(4), Li1a···B1 2.388(4), Li1···Li1a 2.772(4), Li1–H1 1.85(2), Li1–H2A 1.87(2), Li1–H1a 2.04(2), Li1–H5a 2.08(2), B1–H1 1.19(2), B1–H2 1.19(2). Selected bond angles (°): H1–B1–H2 107.3, O1–Li1···B1 139.4(3), O1–Li1···B1A 112.9(5), C9–O1–C11 113.2(7). C5–B1–C1 100.4(5).

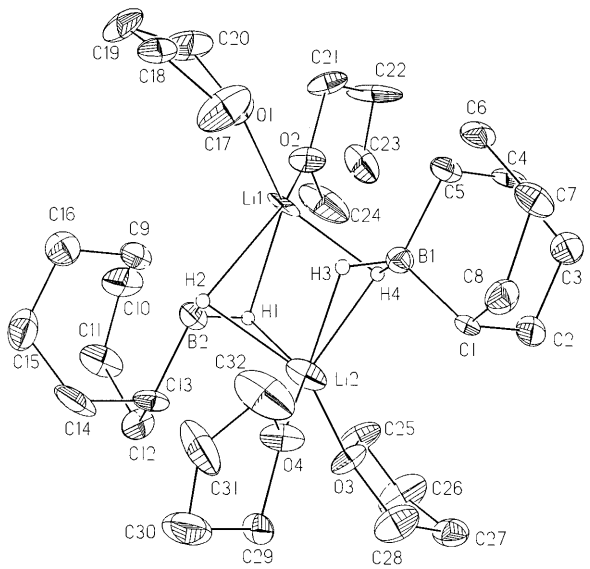

Fig. 8. Molecular structure of dimeric lithium 9-borata-bicyclo[3.3.0]nonane, **6a**·2 THF, in the crystal. Thermal ellipsoid are drawn on a 25% probability scale. Selected atom distances (Å): Li1–O1 1.98(1), Li1–O2 1.98(1), Li2–O3 1.96(1), Li2–O4 1.95(1), Li1–H1 2.18(4), Li1 H2 2.02(5), Li1 H3 2.36(5), Li1 H4 2.00(4), Li1···B1 2.46(1), Li1···B2 2.46(1), Li2···B1 2.49(1), Li2···B2 2.49(1), Li2–H1 2.10(4), Li2–H2 2.09(5), Li2–H3 2.16(3), Li2–H4 2.12(4). Selected bond angles (°): O1–Li1–O2 101.7(4), O3–Li2–O4 102.9(4), Li1···B1···Li2 70.2(2), Li1···B2···Li2 70.2(2), Li1–H1–Li2 83(1), Li1–H2–Li2 88(1), Li1–H3–Li2 78(1), Li1–H4–Li2 87(1), H1–B1–H2 99(2), H3–B2–H4 107(2), C1–B1–C5 106.0(3), C9–B2–C13 105.4(3), C17–O1–C20 107.0(5), C21–O2–C24 106.5(5), C25–O3–C28 108.0(5), C29–O4 C32 107.0(5).

second half of the dimeric unit. Each Li center is penta-coordinated by the oxygen atom of the ether molecule, three H(B) atoms and an agostic Li···H–C bond. The boron atoms have local C_2 symmetry carrying two H atoms and two C atoms with a H–B–H bond angle of 107(2)° and a C–B–C bond angle of 104.2(8)°. One H atom of the H_2B unit binds to two Li centers, the other only to one. Therefore, the H_2BR_2 unit acts as a μ_1^2, μ_1^1 ligand. It should be noted that the Li···H(C) distance is 2.08(2) Å. This distance is not much longer than the longest Li···H(B) distance (2.04(2) Å). The double hydrogen bridge Li1···H1···Li1A is rather asymmetric with bond lengths of 1.85(2) and 2.04(2) Å. Nevertheless, the two Li···B distances are identical within the limits of esd's.

The solvate **6a**·2 THF is much more symmetric than **6a**·OEt_2. As Fig. 8 shows this molecule has two Li centers that are hexa-coordinated by four H(B) atoms and two O atoms of two THF molecules. Therefore, each H_2BR_2 anion acts as a $2\mu_1^2$ unit. While we consider the configuration as being correct, the weakly diffracting crystals allowed only a refinement to $R_1 = 0.12$. Therefore, a more detailed discussion of bonding parameters is not justified.

The solvate (**6a**)$_2$·THF·TMEDA (see Fig. 9) displays an *asymmetric* structure. Firstly, one H atom of each BH_2 group binds to *two* Li centers, the second H atom of each BH_2 group is involved in a single Li···H–B bridge only to atom Li2. Thus, atom Li2 coordinates to four H(B) atoms in addition to two N atoms of the TMEDA ligand. In contrast, atom Li1 coordinates only with two H(B) atoms and the oxygen atom of one THF molecule. In addition, there are two Li···H–C agostic interactions making the Li1 atom penta-coordinated.

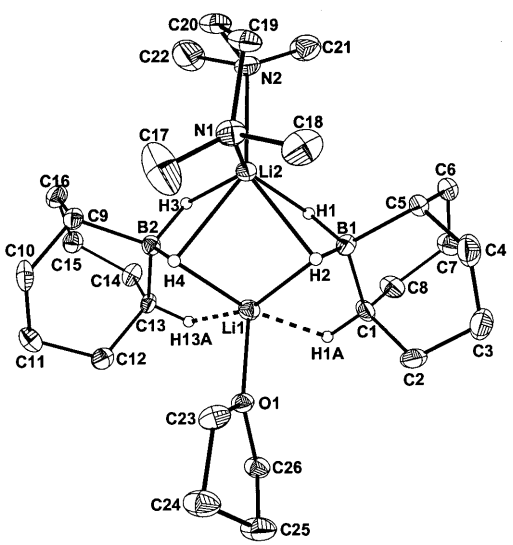

Fig. 9. Molecular structure of the lithium 9-borata-bicyclo[3.3.0]nonane (**6a**)$_2$·THF·TMEDA in the crystal. Thermal ellipsoids are depicted with a 25% probability level. For selected atoms distances and bond angles see Table 4.

The Li_2B_2 unit of $(\mathbf{6a})_2$·THF·TMEDA is not planar but folded with an interplanar angle of 31° for the planes B1Li1B2–B1Li2B2 and 22° for Li1B1Li2–Li1B2Li2. Both Li–N distances (2.119(7), 2.142(7) Å) and the N1–Li2–N3 angle (86.3°) correspond within esd's with those found for dimeric $LiBH_4$·TMEDA [5]. Moreover, also the B1–Li2–B2 angle of 101.9(3)° is practically identical with the B–Li–B angles of 102.4(3)° observed for $(LiBH_4$·TMEDA$)_2$. Due to the smaller H–B–H bond angles in **6a**·2THF the two Li···B distances are slightly longer (2.479, 2.529 Å) than in $(LiBH_4$·TMEDA$)_2$ (aver. 2.464 Å). The main difference to be noted is that the angle between the planes through Li1N1N2 and Li1H1B1H2 or Li1N1N2 and Li1H3B2H4 is ~50° in $(\mathbf{6a}\cdot 2THF)_2$ but 70° for $(LiBH_4$·TMEDA$)_2$. The reason for this difference is due to the different Li···H–B interactions.

The geometry about atom Li1 can be considered to be distorted quadratic pyramidal. The Li1–O1 bond length (1.928(7) Å) is in the expected range [25]. As expected the Li···H(B) bond lengths are shorter (1.88(4) Å) than the Li···H(C) bond lengths (average 2.07(4) Å). This geometry is, therefore, similar to that found for dimeric **6a**·OEt_2.

Compound **4** was obtained as single crystals of the solvate **4**·PMDTA. Its X-ray structure determination shows that dimeric molecules are present in the lattice. Fig. 10 represents its molecular structure. The most

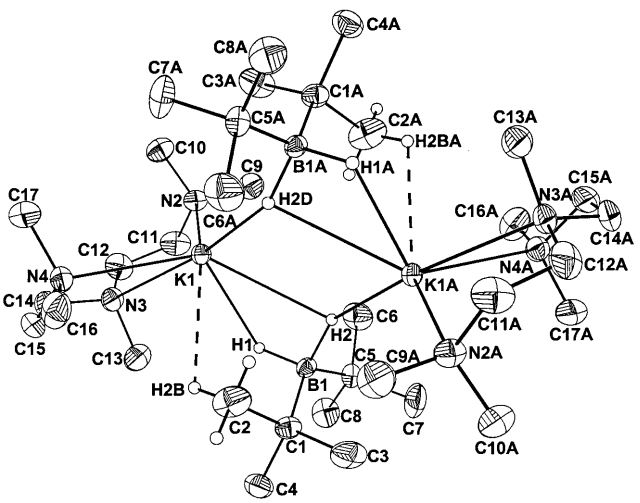

Fig. 10. The molecular structure of dimeric $KH_2B(t\text{-}Bu)_2$·PMDTA, **7·PMDTA** in the crystal. CH hydrogen atoms have been omitted for clarity. Thermal ellipsoids represent a 25% probability level. Selected atom distances (Å): K1–N2 2.947(2), K1–N3 2.949(2), K1–N4 2.956(2), K1···B1 3.292(2), K1–H1 2.56(2), K1–H2 3.06(2), K1–H2D 2.67(1), B1–C1 1.644(3), B1–C4 1.642(3), B1–H1 1.25(2), B1–H2 1.28(1), K1···H2B. Selected bond angles (°): N2–K1–N4 108.85(5), N3–K1–N4 61.73(5), N2–K1–N3 62.38(5), C1–B1–C5 122.7(2), H1–B1–H2 107(2), H1–K1–H2 41.5(4), H1–K1–H2D 69.0, N2–K1–H2 111.4, N2–K1 H2D 125.9, N3–K1–H1 80.9, N3, H1–K1–H2D 109.5, N3–K1–H2 122.3, K1–H2–K1A 111, K1–H1–B1 114.7, K1–H2–B1145.5.

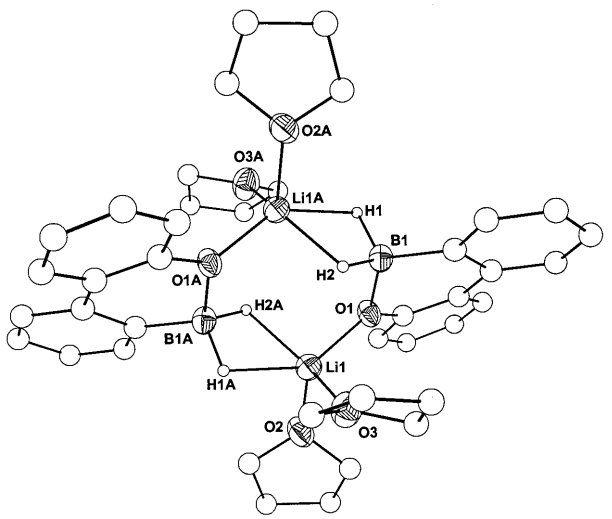

Fig. 11. Molecular structure of dimeric bis(tetrahydrofuran)lithium 6H-dibenzo[c,e][1,2]oxadihydridoborate, **10·2THF**, without CH hydrogen atoms.

significant feature of this molecule is its centrosymmetric structure with an inversion center in the center of the four membered K_2H_2 unit. Each potassium ion coordinates to three H(B) hydrogen atoms and to three nitrogen atoms. In addition, there is a single weak K···H–C interaction. This makes the potassium ion hepta-coordinated. The three K···H distances are quite different with K1–H1 = 2.56(2) Å, K1–H2 = 3.06(2) Å and K1–H2D = 2.67(1) Å and the angle H2–K1–H2D = 41°. Although the B–H distances cannot be accurately determined it follows that they are comparatively

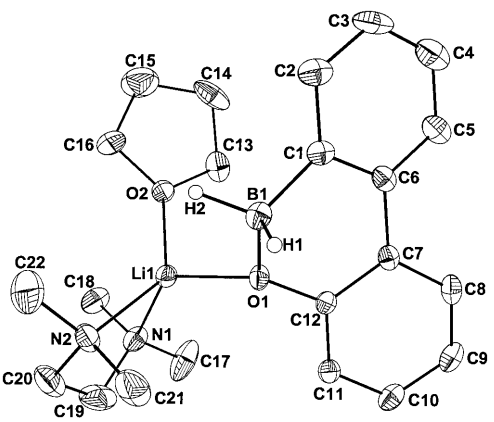

Fig. 12. Molecular structure of tetramethylethylenediamine-tetrahydrofuran lithium 6H-dibenzo[c,e][1,2]oxadihydridoborate, **10·THF·TMEDA**. CH hydrogens have been omitted for sake of clarity. Thermal ellipsoids are depicted at a 25% probability level. Selected atom distances (Å): Li1–O2 1.937(5), Li1–N1 2.155(5), Li1–N2 2.128(5), Li1..B1 2.737(5), Li1–O1 1.535(4) B1–C1 1.588(4), B1–H1 1.14(2), B1–H2 1.14(3). Selected bond angles (°): N1–Li1–N2 85.1(2), O2–Li1–N2 133.9(2), O2–Li1–N1 1000.0(2), O1–Li1–O2 106.0(2), O1–Li1 N1 126.8(2), O1–Li1–N2 106.9(2), C1–B1–O1 108.3(2), H1–B1–H2 109(2), H1–B1–C1 111(1), H1–B1–O1 106(1), H2–B1–O1 106(1), H2–B1–C1 113(1).

long (average 1.265(15) Å) while the H–B–H bond angle of 107(2)° is close to tetrahedral. In contrast, the C1–B1–C4 bond angle is rather open with 122.7(5)° for a tetracoordinated boron atom. This is good indication of strong steric repulsion between the two *tert*-butyl groups. In accord with this are the fairly long B–C bonds (average 1.764 Å, sum of atomic radii: 1.63 Å).

The K–H distances found are shorter (2.67 Å) and longer (3.06(2) Å) as compared to 2.85 Å for potassium hydride KH [26], and similar to the KH distances reported for **17** [27,28]. It follows from the structural data supported by ab initio calculations (v.i.) that compound (**7**·PMDTA)$_2$ has to be considered a tight ion pair.

Compound **10** crystallized as **10**·2THF and as **10**·THF·TMEDA, the former being dimeric in the solid state. Fig. 11 depicts the molecular structure of the THF solvate. In spite of many attempts to grow good diffracting crystals even those displaying a perfect shape were not diffracting well. The best solution converged only at $R_1 = 0.17$. This precludes a discussion of structural details. However, the constitution is well enough established, and even the hydrogen atoms bonded to boron were readily revealed. The dimer of **10**·2THF is centrosymmetric, each lithium center being coordinated to two THF molecules, to two hydrogen atoms of the BH_2 group and to an oxygen atom stemming from the second anion of the dimer which is racemic and possesses axial chirality. The Li centers can be considered to be distorted tetrahedral by three O atoms and taking the boron atom as a coordination center into account. As expected the B1–O1 bond (1.535(4) Å) is shorter than the B1–C1 bond length (1.588(6) Å) but the difference between these two distances (0.053 Å) is shorter than expected on the basis of the atomic radii of the atoms involved.

The heterocyclic anion in **10**·THF·TMEDA (see Fig. 12) adopts a 'pseudo envelope' configuration as revealed by the following torsion angles: C1–C6–C7–C12 = 17.5°, and C1–B1–O1–C12 = 49.1°, i.e. the C1–C6 and the O1–C12 vectors are not parallel to one another. However, the deviation of atoms O1, C1, C6, C7, and C12 from the mean plane is only 0.08 Å while atom B1 is 0.57 Å apart. Inspection of the C–C bonds of the heterocycle reveals alternations between 1.367(4) and 1.469(3) Å indicating C–C bond orders between 1 and 1.5. A comparison of the B–C bond lengths in **10**·THF·TMEDA shows a much shorter bond (1.588(4) Å) as compared to the B–C bond lengths in LiH_2Bfl, **9** (1.610, 1.624 Å). We take this as evidence for less steric strain in **10**·THF·TMEDA, and this is an additional argument for the longer B–C bonds found in $KH_2B(^tBu)_2$ (1.644 Å).

Lithium bis(benzenedithiolato)borate crystallized from THF as **17**·2 THF which also proved to be dimeric in the solid state. It is a centrosymmetric molecule, its structure being shown in Figs. 13 and 14, the latter giving a view of the core structure. which can be considered a double cubane unit with two of the opposing edges missing.

The planes comprising atoms Li1S1B1S3 and B1S1Li(1A)S4 stand almost perpendicular to the Li1S1B(1A)S(1A) plane (88, 92°). Each Li ion is hexacoordinated by four S atoms and two O atoms of the THF solvated molecules which are present in cis position. The O2L1S2 plane is quite close to be really planar because the sum of bond angles is 360.8°.

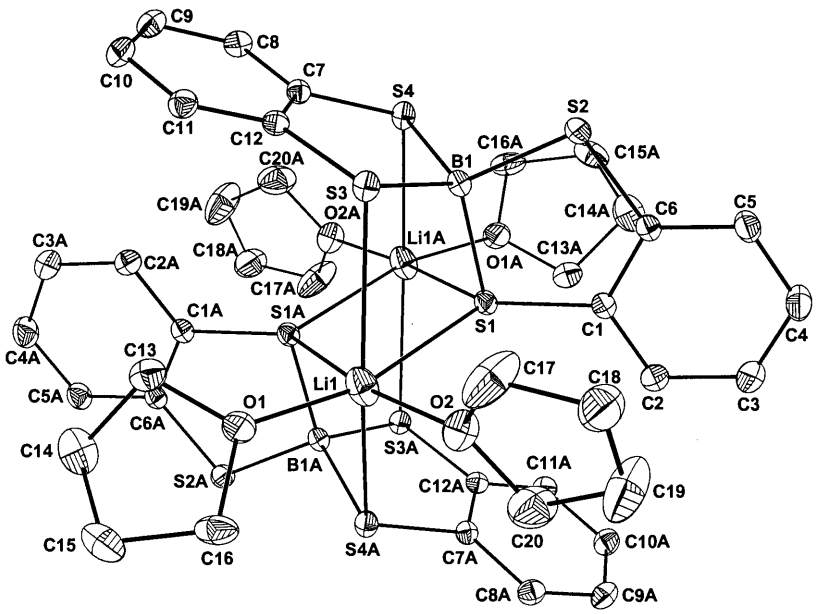

Fig. 13. Overview of the molecular structure of lithium bis(benzo-1,2-dithiolato)borate tetrahydrofuran.

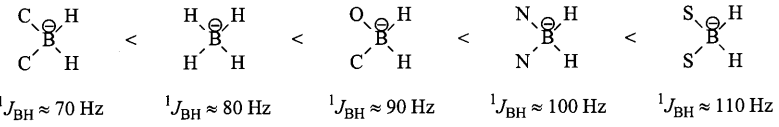

Scheme 1. $^1J(^{11}B^1H)$ coupling constants for dihydrido borates $H_2BX_2^-$.

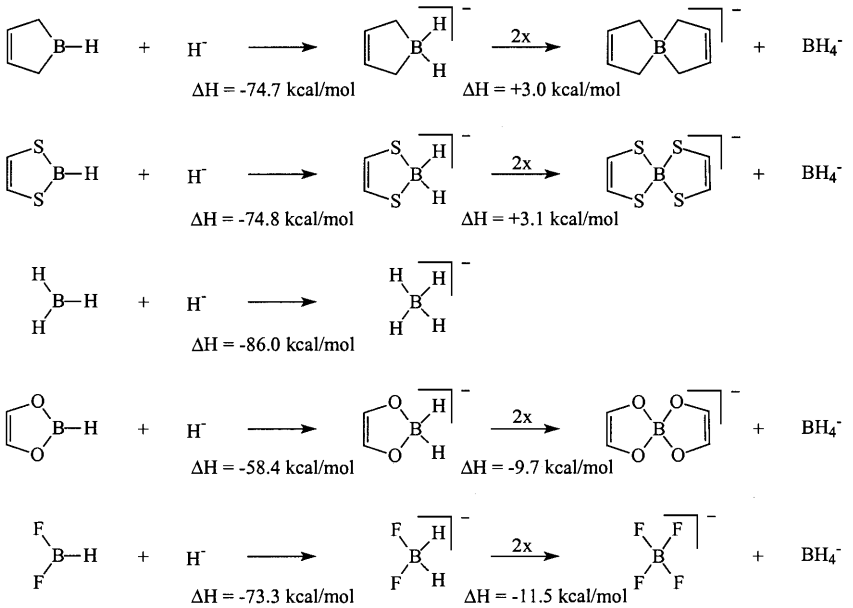

Scheme 2.

Nevertheless, looking at the Li–S bond lengths one finds that these are unusually long, and, moreover, quite different, ranging from 2.744(6) Å to 2.934(8) Å. Atom distances between dicoordinated S and tetracoordinated B atoms are about 0.03 Å shorter compared to tricoordinated S atoms. S–B–S bond angles in (**17**·2 THF) $_2$ are close to 104° while the S–Li–S bond angles cover the wide range from 66.7° (S4A–Li1–S1A) to 147.8(2)° (S3–Li1–S4A). The largest bond angle is 162.0(3)° for O2–Li1–S1A. Therefore, the bond angles demonstrate that the 'cubane' unit is strongly distorted.

5. Discussion

Although dihydrido diorganyl borates of lithium and potassium can be comparatively readily prepared by reactions delineated in Eqs. (1)–(3) there is evidence that they suffer H^-/R^- exchange, particularly with formation of RBH_3^- species. Surprisingly no R_3BH^- or BR_4^- ions could be detected in the solutions by ^{11}B-NMR spectroscopy, but $LiBH_4$. In the synthesis of $Li[H_2B(C_5H_9)_2]$, **5**, a ratio of 64:23:13 for **5**: $Li(H_3BC_5H_9)$: $LiBH_4$ was observed. In the case of $Li(H_2BMe_2)$ the ratio of **1**:**2** was 9:1 for the diethyl ether solution. Previously a mixture consisting of **2**, **1** and $Li(HBMe_3)$ was found for a THF–hexane solution [17]. On the other hand, the presence of the bulky *tert*-butyl group or the incorporation of the boron atom in a ring system (thexylborane [14], disiamylborane [15], 9-borabicyclononane [14], 9-borafluorene, isopinocamphylborane [15]) obviously retards or even prevents the hydride–organyl exchange. Even more pronounced is this ligand redistribution for dihydrido diorganyloxo borates e.g. **11** and their thiolato analogues as represented by Eq. (5). So far, no alkali metal dihydrido catecholato borate could isolated or even be detected by ^{11}B-NMR in solution [21]. In this respect the sulfur analogue behaves better because anions of type $H_2B(S_2R)^-$, **14** and **15**, were found to be the main species in solution by reacting $LiBH_4$ with dithiols. However, in the case of dithiocatechol compound **14** was observed and could even be isolated, as well as $LiB(S_2C_6H_4)_2$ which crystallized from a THF solution as dimeric **17**·2THF. At the moment we can only speculate on the process of the ligand redistribution because we cannot distiguish between a process that starts from a $H_2BR_2^-$ species or from a process involving hydride attack on the borane starting material where a R_2BH species is a most likely intermediate.

In order to learn about the thermodynamics of the redistributions in analogy to Eqs. (4) or (5) calculations have been performed for $H_2BX_2^-$. The results are summarized in Scheme 1.

These calculations (performed on a B3LYP/6-311 + G(2df,2p)//B3LYP/6-31G(2d,p)-level) [29] show that

the hydride affinity of a borane X_2BH as depicted in Scheme 2 range from -58.4 to -74.8 kcal mol^{-1}. According to these data BH_3 has the highest hydride affinity followed by the dithioborolene. However the driving force for the ligand exchange depends on the electronegativity of the boron substituents X in the anions $X_2BH_2^-$. The calculations lead to the order $F^- > RO^- > Me^- > RS^-$. Large energy differences for this process could not be expected because the number of bonds to the boron atoms does not alter during ligand exchange. The energy data may change of course when borate–cation interactions are taken into account.

X-ray structure information on dihydrido diorganyl borates exists so far only for zirconium and niobium complexes (**22**–**28**) with the exception of $Li(H_2Bmes_2)$·DME [9] for a lithium compound. All these compounds contain doubly hydrogen bridged H_2BR_2 groups, and only **24** contains one of these group *singly bridged*. However, as our results show, the diydrido diorganyl borate is a much more flexible ligand and adopts various kinds of coordination in dinuclear molecular species. Mononuclear **9**·3THF exhibits the 'usual' double hydride bridge with an Li···B distance of 2.454(4) Å. Its B–C bonds (1.624, 1.610(3) Å) are of the same length as found for the potassium salt **28** (1.62(1) Å) [27] and are somewhat shorter than for $Li(H_2Bmes_2)$·2 DME (1.640(5) Å) [9] while a significantly shorter B–C bond has been determined for the doubly reduced borole species **29** (1.53 Å) [27]. The latter is the consequence of the formation of a 6π-electron species.

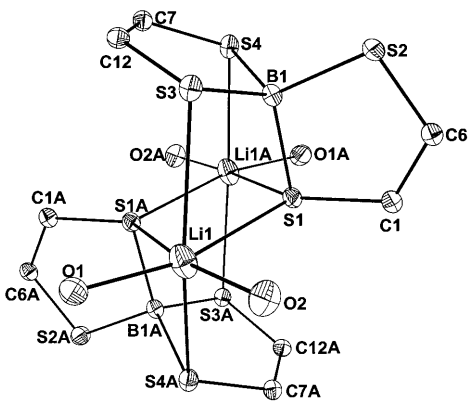

Fig. 14. The core structure of **17·2 THF**. Thermal ellipsoids are drawn on a 25% probability scale. Selected bond lengths (Å): B1–S1 1.930(4), B1–S2 1.901(4), B1–S3 1.932(4), B1–S4 1.928(4) Li1–O1 1.904(7), Li1–O2 1.936(7) Li1–S1 2.744(6), Li1 S3 2.813(8), Li1–S1A 2.879(7), Li1–S4A 2.934(8). Selected bond angles (°): S1–B1–S2 104.0(3), S2–B1–S3 112.2(2), S1–B1–S3 114.4(2), S2–B1–S4 112.0(2), S1–B1 S4 112.0(2), S3 B1 S4 104.4(2), O1–Li1–O2 104.0(3), O1–Li1–S1 161.2(4), O1–Li1–S1A 93.5(3), O1–Li1–S3 102.6(3), O2–Li1–S1 94.3(3), O2–Li1–S1A 161.0(3), O2–Li1–S3 98.2(3), S1–Li1–S4A 85.1(2), S1–Li1–S3 70.0(2), S1–Li1–S1A 69.0(2), S3–Li1–S4A 147.8(2), S3–Li1–S1A 85.0(2), S1A–Li1–S4A 66.7(2).

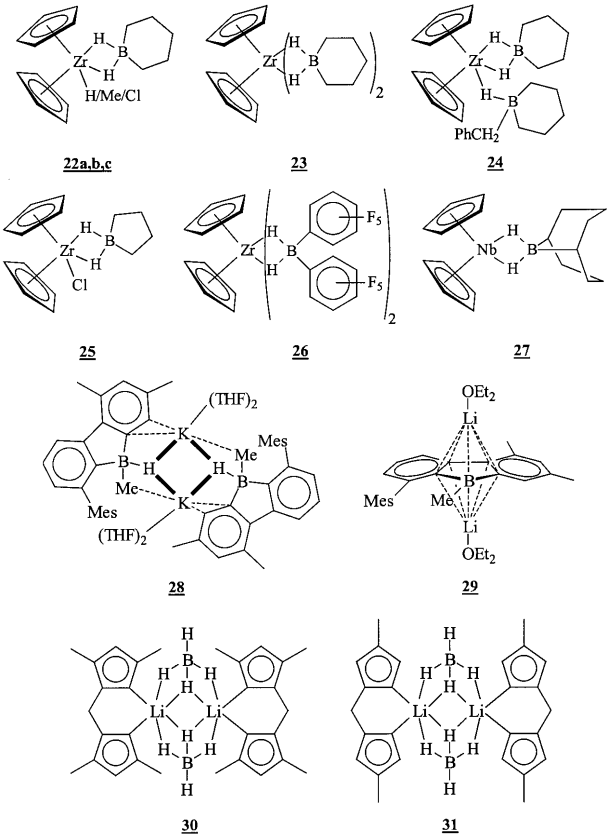

The influence of the auxiliary ligands on the structure becomes evident for the various solvates of compound **6a**. Since all of them are dinuclear they are good examples for comparison. Each H_2BR_2 group provides a doubly bridging H(B) atom besides a singly bridging one. The coordination sphere is completed by a Li···H(C) agostic interaction. The Li–H distances show that the Li···H(C) interaction (2.08 Å) is almost as strong as the weakest Li···H(B) bond (2.04 Å). Since the anion of **6a** coordinates via its two H(B) atoms to Li one might expect a Li···B atom distance that is typical for a LiH_2B bridge. Actually, the observed Li···B distances (2.388, 2.392 Å) are shorter than in $Li(H_2Bmes_2)$ [9], and even slightly shorter than in **9**·3THF.

In dimeric **6a**·2THF we also find four hydrogen atoms to be coordinated to the hexa-coordinated Li centers, however, there are no Li···H(C) interactions. The Li···B distances are slightly longer (average 2.47 Å) than for the ether solvate, and this may be due to the higher coordination number. The fact that all H(B) atoms form Li···H···Li bridges is so far a rare example for hydridoborates. This kind of interaction is also present in $(\mathbf{6a})_2$·THF·TMEDA for the TMEDA carrying Li atom, which is hexa-coordinated. The second Li atom which coordinates to the THF molecules has only two Li···H–B bonds but, in addition it complete its coordination sphere by two agostic Li···H–C interac-

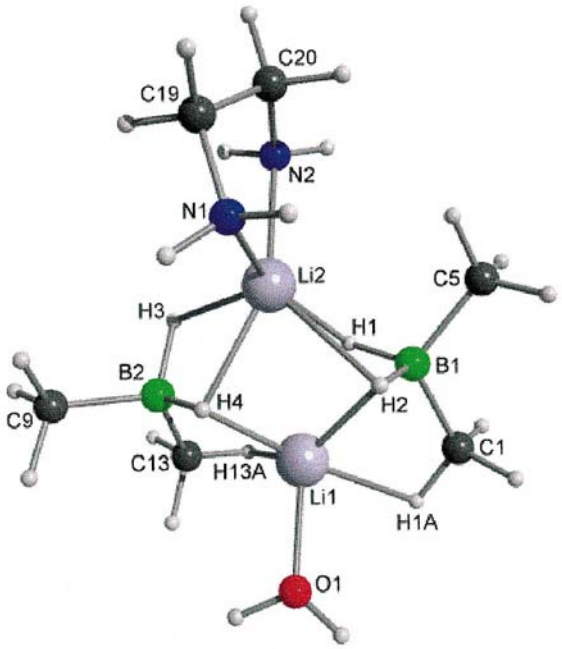

Fig. 15. Calculated structure for model compound **21** (= 2 $LiBH_2Me_2{\cdot}OH_2{\cdot}$en).

tions. In this case, the Li···H(C) distances are longer (2.08, 2.05 Å) than the longest Li···H–B distances (1.86, 1.89 Å). The asymmetry of the molecule is reflected also in the Li···B atom distances which are shorter for Li1 (2.365, 2.380(9) Å) than for Li2 (2.479, 2.529(8) Å).

The observed structure for $(\mathbf{6a})_2{\cdot}$THF·TMEDA is verified by ab initio calculations for the model compound **22** = (**1**·OH_2en) (at DTF level, B3LYP optimized with a 6-31G(d,p) basis set) as depicted in Fig. 15. Table 4 reveals a good correlation between the bonding parameters for the model and the $(\mathbf{6a})_2{\cdot}$THF·TMEDA counterpart. According to the NBO analysis [29] the model system has to be described by localized wave functions, e.g. the solvates of the alkali metal dihydrido diorganyl borates have to be described as ion pairs. The energy contributions to the stability of these molecules results primarily from the donor function of N and O atoms to the Li cation. Average energy contributions are as follows: Li2–N1(lp) 11.6 kcal mol^{-1}, Li2–(H1,3)B = 7.1 kcal mol^{-1}, Li2–H2(B) 4.9 kcal mol^{-1}, Li1–O1(lp) 19.8 kcal mol^{-1}, Li1–H2,4(B1) = 8.2 kcal mol^{-1}, Li1–H1A(C) 3.4 kcal mol^{-1} (lp = lone pair). Thus the energy contribution by the Li···H(C) bond is rather small.

$K[H_2B(^tBu)_2]$ crystallizes as dimeric **4**·PMDTA in spite of the bulky tridentate amine ligand. The coordination sphere around K is completed by three H(B) hydrogen bridges and one H(C) bridge. K–H distances span the wide range from 2.56 to 3.06 Å, with the K···H(C) distance lying in between (2.67(1) Å). Similar K–H parameters are reported for dimeric $K(HMeBmes_2){\cdot}2$THF, **27**, the H(B) atom bridges to two potassium cations. [25] In this case the K···H···K bridges are more symmetric (2.57. 2.74 Å) than in **4**·PMDTA. In both compound the potassium center is hepta-coordinated.

Although the trihydridomethylborate **2**·2THF is also dimeric its structure resembles the structure of dimeric $LiBH_4{\cdot}$TMEDA with a $\mu_1^2,2\mu_1^1$ H_3B function. This bonding pattern has also been observed for **30** and **31** having Li···B distances longer than in dimeric $LiBH_4{\cdot}$TMEDA (2.461(6), 2.467(5) Å) [5]. The particularly long Li···B distance in **30** (2.584 Å) is probably due to steric repulsion by the methyl groups in 3-posi-

Table 4
Experimentally determined selected bonding parameters of compound $(\mathbf{6a})_2$ THF TMEDA and calculated parameters for the model compound $LiMe_2BH_2{\cdot}OH_2{\cdot}(H_2NCH_2CH_2NH_2)$ [a]

Bond lengths					
B1–H1	1.17(4) (1.253)	B2–H3	1.20(4) (1.243)	Li2–H1	1.93(4) (1.919)
B1–H2	1.14(4) (1.253)	B2–H4	1.13(3) (1.257)	Li2–H2	2.16(4) (2.243)
B1–C1	1.627(6) (1.645)	B2–C9	1.617(6) (1.627)	Li2–H3	1.94(4) (1.902)
B1–C5	1.611(6) (1.626)	B2–C13	1.626(6) (1.651)	Li2–H4	2.19(3) (2.085)
Li1–H2	1.89(4) (1.914)	Li1–B1	2.300(9) (2.212)	Li2–B1	2.479(8) (2.478)
Li1–H4	1.86(3) (1.818)	Li1–C1	2.502(9) (2.516)	Li2–B2	2.529(8) (2.471)
Li1–H1A	2.08(4) (2.161)	Li1–C13	2.524(8) (2.389)	Li2–N1	2.142(7) (2.103)
Li1–H13A	2.05(4) (2.097)	Li1–O1	1.928(7) (1.945)	Li2–N2	2.119(7) (2.115)
Li1–B2	2.365(9)(2.431)				
Bond angles					
H1–B1–H2	105(3) (105.31)	H3–B2–H4	106(2) (105.93)		
C1–B1–C5	105.6(4) (112.82)	C9–B2–C13	105.2(3) (112.61)		
O1–Li1–H2	106(1) (112.29)	O1–Li1–H4	105(1) (101.43)		
O1–Li1–H1A	90(1) (84.01)	O1–Li1–H13A	98(1) (107.13)		
H2–Li1–H4	92(2) (87.25)	H4–Li1–H13A	83(2) (93.05)		
H1A–Li1–H13A	94(2) (88.12)	H1A–Li1–H2	84(2) (87.91)		
B1–Li2–B2	101.9(3) (104.97)	N1–Li2–N2	86.3(3) (84.65)		

[a] Optimized structure using the B3LYP/6-31G(d,p) basis set (*C*1 symmetry).

tion of the pyrazole rings, because in **31** the Li···B distances are shorter, ranging from 2.407(9) to 2.498(9) Å [30].

The structural parameters of alkali metal hydridoborates allow a distinction between LiH_3B and LiH_2B bonding patterns. The Li··B distances for the latter are in the range for mononuclear and dinuclear lithium hydrido borates (2.40–2.53 Å), while for triply bridged species the range is 2.25–2.35 Å. This fits with Edelstein's rules [31] and is, of course, a consequence of the geometry of the 'tetrahedral' hydrido borate species, e.g. the orientation of the BH_4^-, RBH_3^- and $R_2BH_2^-$ to the alkali metal center.

6. Experimental

Since most compounds are more or less moisture and air sensitive the Schlenck technique has been used throughout by using nitrogen as a protecting gas. Flame dried glassware was employed and for particularly sensitive materials the glassware was treated with Me_3SiCl to remove adsorbed water and to protect OH groups.

The reactions were monitored by NMR methods, particularly ^{11}B-NMR. Bruker AP 200 and JEOL 270 and 400 instruments were used for recording ^{11}B-, ^{1}H-, and ^{13}C-NMR spectra. TMS, and $F_3B{\cdot}OEt_2$ were used as standards, and C_6D_6 and $CDCl_3$ were employed as solvents besides others (as quoted). Positive δ values refer to lower frequencies than the standard (higher field). C atoms bonded to boron atoms could in most cases not be recorded under standard conditions due to quadrupolar relaxation effects. IR spectra were recorded using a Jeol FT IR instrument. Elemental analysis were performed at the departments microanalytical laboratory.

6.1. Starting materials

Commercial grade chemicals were LiH, NaH, KH, $LiBH_4$, $NaBH_4$, LiBu in hexane, LiMe in ether, catechol, 1,2-benzenedithiol, 1,2-ethanedithiol and ephedrine. The following compounds were prepared by literature methods: Me_2BBr [32], 6-chloro-6H-dibenzo-[c,e][1.2]-oxaborane [33], 9-borabicyclo[3.3.1]nonane [34] dimer, lithium bis(cyclohexyl)dihydridoborate [35], $^tBu_2BCl$ [36], 9-Cl-9-borafluorene [37].

6.2. Lithium dihydrido dimethyl borate, (*1*) and lithium methyl trihydrido borate-2-tetrahydrofuran (*2*·2 THF)

Lithium hydride (2.19g, 276 mmol) was suspended in tetrahydrofuran (40 ml). After cooling to −78°C dimethylboron bromide (5.90 g, 48.8 mmol) dissolved in pentane (40 ml) was slowly added to the stirred suspension. After the addition was complete the mixture was allowed to attain ambient temperature. Stirring was then continued for additional 2 h. The solution showed the following ^{11}B-NMR signals at that time: $\delta = -31.6$ (quart., $^1J(^{11}B^1H) = 74$ Hz (**2**)) and −23.9 (t, $^1J(^{11}B^1H) = 70$ Hz (**1**)); ratio = 1:9.

Insoluble material was filtered off and the solution reduced in vacuo to about 30 ml. Storing the solution at −30°C produced clear crystals showing two different kinds of habitus of which only one sort of these (needles) was suitable for X ray structure analysis and were shown to be $Li(MeBH_3)\cdot 2THF$. No elemental analysis was performed due to 'explosive' combustion. Selected needles gave the following NMR data: ^{1}H-NMR (400 MHz, C_6D_6): $\delta = 0.50$ (br. s, 6H, $(H_3C)_2BH_2Li$), 1.08 (q, $^1J(^{11}B,^1H) = 70$ Hz, $(H_3C)_2BH_2Li$), 1.37 (m, 4H, C_4H_8O), 3.73 (m, 4H, C_4H_8O);

6.3. Lithium dihydrido borepinate (*8*)

1,5-Hexadiene (18.9 ml, 159 mmol) was dissolved in THF at 0°C. To this stirred solution was added a solution of BH_3 in THF (50 ml, 2.12 M, 106 mmol). After stirring for an additional 1 h at 20°C the solvent was removed in vacuo. An oily residue remained which was heated to 160°C for 3 h. The colorless liquid was dissolved in THF (40 ml), and additional BH_3 in THF (25 ml, 1.21 M, 53 mmol) was dropwise added and the resulting solution stirred for 16 h. LiH powder (2.3 g, 289 mmol) was then added and stirring was continued for 1 h. Excess LiH was then removed by filtration. The solution showed the following NMR signals: ^{11}B-NMR (64 MHz, THF): $\delta = -26.1$ (q, $^1J(^{11}B,^1H) = 75$ Hz, LiH_3B–$(CH_2)_6$–BH_3Li, 28%), −16.4 (t, $^1J(^{11}B,^1H) = 71$ Hz, $(CH_2)_6BH_2Li$, 72%). All volatile material was removed from the solution at 1 Torr, and the colorless residue dissolved in a mixture of hexane and THF (70 and 30 ml). No separation of the two compounds by fractional crystallization was possible.

6.4. Potassium salt

Three milliliters of the solution of **8** was treated with about 10 mg of KH in an NMR tube. After 1 h the following NMR signals were observed: ^{11}B-NMR (64 MHz, THF): $\delta = -28.2$ (q, $^1J(^{11}B,^1H) = 75$ Hz, KH_3B–$(CH_2)_6$–BH_3K, 26%), −18.2 (t, $^1J(^{11}B,^1H) = 71$ Hz, $(CH_2)_6BH_2K$).

6.5. Lithium dihydrido borata-bicyclo[3.3.0]nonane (*6a*)

(a) 10.25 g of dimeric 9-borabicyclononane (42 mmol) were dissolved in diethyl ether (100 ml) and a suspension of finely ground LiH (200 mmol) in ether

was added to the borane. After stirring over night and heating to reflux for 4 h all insoluble material was removed by filtration. On cooling the solution to −30°C clear crystals separated suitable for an X-ray structure determination. They proved to be **6a**·OEt_2. The yield of the crystals was not determined.

(b) Dimeric 9-borabicyclononane (20.5 g, 84.0 mmol) was dissolved in THF (200 ml). A THF suspension of LiH (30 ml, 3.02 g, 380 mmol) was added to the stirred solution. A slightly exothermic reaction occurred, and after stirring for 1 h the insoluble material was removed by filtration. After removal of all volatile material from the filtrate the remaining white solid was washed with hexane, m.p. 72–87°C. Yield 33.1 g (94%).

Single crystals separated from a saturated THF solution (ambient temperature) after cooling to −30°C within a few days. The crystals were suitable for an X-ray structure determination and proved to be dimeric **6a**·2THF.

About 1 g of **6a**·2THF was dissolved in THF and several drops of TMEDA were added. Colorless crystals formed on standing for three days. These single crystals proved to be (**6a**)$_2$·THF·TMEDA. ^{1}H-NMR (400 MHz, C_6D_6): $\delta = 0.94$ (q, 4H, $^1J(^{11}B,^1H) = 71$ Hz, $C_8H_{14}BH_2Li$), 1.33 (m, 2H, $C_8H_{14}BH_2Li$), 1.42 (m, 4H, C_4H_8O), 1.71 (s, 4H, –CH_2–$N(CH_3)_2$), 1.85 (s, 12H, –CH_2–$N(CH_3)_2$), 2.16–2.28 (m, $C_8H_{14}BH_2Li$), 2.38–2.49 (m, $C_8H_{14}BH_2Li$), 2.52–2.78 (m, $C_8H_{14}BH_2Li$), 3.52 (m, 4H, C_4H_8O); $^{13}C\{^1H\}$-NMR (100 MHz, C_6D_6): $\delta = 25.37$ (C_4H_8O), 27.12 ($C_8H_{14}BH_2Li$), 36.36 ($C_8H_{14}BH_2Li$), 45.17 (–CH_2–$N(CH_3)_2$), 56.25 (–CH_2–$N(CH_3)_2$), 67.98 (C_4H_8O).

6.6. Lithium bis(cyclopentyl) dihydrido borate (5)

Cyclopentene (7.49 g, 110. mmol) dissolved in THF (50 ml) was hydroborated with BH_3 dissolved in THF (25 ml, 2.2 M, 55 mmol) at 0°C. Stirring was continued at ambient temperature for 2 h. A voluminous precipitate formed. LiH (0.95 g, 120 mmol) was added to the suspension. The precipitate dissolved and the excess of LiH was filtered off after 2 h. According to the ^{11}B-NMR spectrum of the clear solution a mixture of $LiH_2B(C_5H_9)_2$, **5**, $LiH_3BC_5H_9$ and $LiBH_4$ had formed in the ratio of 64:23:13.

^{11}B-NMR (64 MHz, THF): $\delta = -41.2$ (quint, $^1J(^{11}B,^1H) = 81$ Hz, $LiBH_4$, 13%), −25.9 (q, $^1J(^{11}B,^1H) = 75$ Hz, $C_5H_9BH_3Li$, 23%), −14.1 (t, $^1J(^{11}B,^1H) = 68$ Hz, $(C_5H_9)_2BH_2Li$, 64%).

Attempted separation of the species from solutions with different ratios of hexane and diethyl ether for fractional crystallization failed.

6.7. Potassium di-tert-butyl dihydrido borate (4)

A solution of $(Me_3C)_2BCl$ (6.94 g, 43.2 mmol) in THF (50 ml) was added at 0°C to a suspension of KH (4.26 g, 106 mmol) in THF (20 ml). After stirring for 18 h at 0°C all insoluble material was filtered off, and the solvent removed from the solution in vacuo. A solid remained which was heated at 0.1 Torr at 60°C to remove as much coordinated THF as possible. The white solid **4** showed a m.p. of 152–154°C. Yield: 6.74 g (94%).

$C_8H_{20}BK$ (166.16): Anal. Found: C, 56.62; H, 11.30. Calc. for C57, 83; H, 12.13%.

^{1}H-NMR (400 MHz, C_6D_6): $\delta = 0.27$ (q, 2H, $^1J(^{11}B,^1H) = 71$ Hz $C_8H_{18}BH_2$), 1.14 (s, 18H, $C_8H_{18}BH_2$); $^{13}C\{^1H\}$-NMR (100 MHz, C_6D_6): $\delta = 35.74$ ($C_8H_{18}BH_2$); ^{11}B-NMR (64 MHz, C_6D_6): $\delta = -2.8$ (t, $^1J(^{11}B,^1H) = 71$ Hz, $C_8H_{18}BH_2$); IR (THF): $\tilde{\nu} = 2094$ (st, asym. B–H^b), 2167 (st, sym. B–H^b) cm^{-1}.

4 (0.5 g) was dissolved in a minimum amount of toluene. About 3 ml of pentamethyl-diethylenetriamine was added. Single crystals which proved to be dimeric $KH_2B(^tBu_2)$·PMDTA separated on storing the mixture at 0°C for several days.

6.8. Lithium 9,9-dihydrido-9-borataf luorene-3-tetrahydrofuran (9·3THF)

To a stirred suspension of LiH in THF (0.46 g, 58 mmol; 50 ml) was added dropwise a solution of 9-chloro-9-borafluorene (2.17 g, 10.9 mmol) in pentane (40 ml). The reaction was slightly exothermic. Two hours later all insoluble material was filtered off and the solvents removed in vacuo (0.1 Torr). Crystallization from toluene–THF yielded **9**·3THF (3.98 g, 94%); m.p. 87–89°C.

$C_{24}H_{34}BLiO_3$ (388.28); Anal. Found: C, 73.33; H, 8.53. Calc. for C, 74.24; H, 8.83%.

^{1}H-NMR (400 MHz, $CDCl_3$): $\delta = 1.82$ (m, 12H, C_4H_8O), 1.98 (q, 2H, $^1J(^{11}B,^1H) = 77$ Hz, $C_{12}H_8BH_2$), 3.69 (m, 12H, C_4H_8O), 7.10 (t, 2H, $^3J(^1H,^1H) = 7.0$ Hz, $C_{12}H_8BH_2$), 7.17 (t, 2H, $^3J(^1H,^1H) = 7.1$ Hz, $C_{12}H_8BH_2$), 7.59 (d, 2H, $^3J(^1H,^1H) = 6.6$ Hz, $C_{12}H_8BH_2$), 7.74 (d, 2H, $^3J(^1H,^1H) = 7.5$ Hz, $C_{12}H_8BH_2$); $^{13}C\{^1H\}$-NMR (100 MHz, $CDCl_3$): $\delta = 25.54$ (C_4H_8O), 68.39 (C_4H_8O), 119.14, 124.47, 124.98, 131.19, 149.81 ($C_{12}H_8BH_2$); ^{11}B-NMR (128 MHz, $CDCl_3$): $\delta = -22.3$ (t, $^1J(^{11}B,^1H) = 78$ Hz, $C_{12}H_8BH_2$); IR (Nujol): $\tilde{\nu} = 2211$ (st, asym. B–H^b), 2251 (st, sym. B–H^b), additional band at 2074 (w), 2124 (m) cm^{-1};

6.9. Lithium 6H-dibenzo[c,e]oxadihydridoborate-2 tetrahydrofuran (10·2THF)

Prepared as for **9** from LiH (0.29 g, 36 mmol) in THF (50 ml) and 6-chloro-6H-dibenzo[c,e]oxaborane (1.69 g, 7.88 mmol) in THF (40 ml). After most of the solvent had been removed toluene (80 ml) was added to the residue. The insoluble compound was filtered off and washed several times with a mixture of toluene and THF (5 + 1). Drying the solid at 0.1 Torr yielded 1.91 g (73%) of **9**·2 THF. Crystallization from THF produced clear

single crystals of **9**·2 THF, m.p. 75–58°C. No impurities were detected by NMR. Elemental analysis gave variable results due to loss of THF on weighing. ^{1}H-NMR (400 MHz, D_8-THF): $\delta = 1.76$ (m, 8H, C_4H_8O), 3.42 (m, 8H, C_4H_8O), 7.02 (t, 1H, $^3J(^1H,^1H) = 7.5$ Hz, $C_{12}H_8OBH_2$), 7.15 (d, 1H, $^3J(^1H,^1H) = 7.7$ Hz, $C_{12}H_8OBH_2$), 7.23 (t, 1H, $^3J(^1H,^1H) = 7.5$ Hz, $C_{12}H_8OBH_2$), 7.30 (t, 1H, $^3J(^1H,^1H) = 7.2$ Hz, $C_{12}H_8OBH_2$), 7.51 (t, 1H, $^3J(^1H,^1H) = 7.5$ Hz, $C_{12}H_8OBH_2$), 8.09 (d, 1H, $^3J(^1H,^1H) = 7.8$ Hz, $C_{12}H_8OBH_2$), 8.10 (d, 1H, $^3J(^1H,^1H) = 7.8$ Hz, $C_{12}H_8OBH_2$), 8.40 (d, broad, 1H, $^3J(^1H,^1H) = 6.0$ Hz, $C_{12}H_8OBH_2$); $^{13}C\{^1H\}$-NMR (100 MHz, D_8-THF): $\delta = 25.53$ (C_4H_8O), 67.70 (C_4H_8O), 120.32, 121.45, 121.87, 124.39, 124.49, 127.18, 129.16, 131.31, 135.87, 141.58, 155.67 ($C_{12}H_8OBH_2$); ^{11}B-NMR (64 MHz, THF): $\delta = -3.9$ (t, $^1J(^{11}B,^1H) = 91$ Hz, $+40$°C, $C_{12}H_8OBH_2$); IR (THF): $\tilde{\nu}$2170 (m), 2238 (st), 2247 (st), 2289 (st), 2369 (w) cm^{-1}; (Nujol): $\tilde{\nu}$2068 (st), 2091 (m), 2134 (st), 2170 (st), 2204 (m), 2226 (m), 2271 (st), 2295 (st), 2355 (w), 2417 (w) cm^{-1}; Crystallization of **10**·2THF from a THF solution in the presence of TMEDA produced crystals of composition **10**·THF·TMEDA.

9-Chloro-6H-dibenzo[c,e]oxaborane did not react with KH within 16 h in THF solution. Only the formation of 6H-dibenzo[c,e]oxaborane but not the dihydridoborate was noted by ^{11}B-NMR spectroscopy ($\delta = 28.5$, broad, BH coupling could not be resolved).

6.10. Reaction of Lithium o-hydroxy-phenolate with BH_3THF in THF

Catechol (0.33 g, 2.0 mmol) was dissolved in THF (20 ml). This solution was dropped into a stirred solution of LiBu in hexane (20.0 ml, 1.55 mmol). After the gas evolution had ceased stirring was continued for 30 min. The solution was then cooled to 0°C and a solution of BH_3 in THF (21.4 ml, 3.08 mmol) was added. After warming to ambient temperature the ^{11}B-NMR investigation of the solution showed signals at -40.8 (quint., $^1J(^{11}B,^1H) = 81$ Hz; $LiBH_4$), 9.0 (broad, h(1/2) = 180 Hz), and 11.9 (s, $LiB(O_2C_6H_4)_2$), **16**, were present in a ratio of 4:3:4.

6.11. Reaction of $LiBH_4$ with 1,1-di(2-hydroxy-3-tert-butyl-5-methylphenyl)methane (12)

A solution of $LiBH_4$ (0.25 g, 11.5 mmol) in THF (30 ml) was cooled to 0°C. While stirring a solution of 1,1-di(2)-hydroxy-3-*tert*-butyl-5-methylphenyl)methane (3.91 g, 11.9 mmol) was added dropwise. After the gas evolution had ceased the solution was allowed to attain ambient temperature. ^{11}B-NMR spectroscopy showed the presence of two species: $LiBH_4$ ($\delta = -41.5$, quint., $^1J(^{11}B,^1H) = 81$ Hz) and $LiB(OAr)_4$, ($\delta = 3.7$); ratio = 1:1 but not of the expected compound **12**.

6.12. Reaction of KH with [4S,5R]-3,5-dimethyl-4-phenyl[1.3.2]oxazaborolidine in the presence of 18-crown-6

KH (860 mg, 21.5 mmol) was suspended in THF (30 ml) and the crown ether added (5.67 g, 21.5 mmol). To the stirred suspension was dropped a solution of the borolidine **19** (3.37g, 19.2 mmol) in THF (50 ml). After 3 days the B-NMR spectrum showed signals at -10.7 (broad, H_2BN_2 moiety of **20**), 0.6 ppm (t, $^1J(^{11}B,^1H) =$ 90 Hz, $NOBH_2$ moiety of **13**, and 10.6 ppm (N_2BO_2 moiety of **20**). The crown ether complex of **13** could not be separated from the mixture.

6.13. Lithium dihydrido-1,3,2-benzenethiolatoborate (14)

To a stirred solution of $LiBH_4$ (139 mg, 6.38 mmol) in THF (30 ml) was added at 0°C a solution of 1,2-benzodithiol (907 mg, 6.38 mmol) in THF (30 ml). After the hydrogen evolution had ceased stirring was continued for additional 4 h. Then the solvent was removed in vacuo (0.1 Torr). **14** remained as a colorless solid, m.p. 79–81°C; yield: 1.81 g (93%). NMR data showed that the compound contained only trace impurities.

In order to get single crystals of **14** the material was crystallized form a mixture of THF and toluene (1:1) at 50°C. This solution showed three ^{11}B-NMR signals due to $LiBH_4$ [$\delta = 40.9$, quint.], $LiH_2BS_2C_6H_4$, **14**, [-11.0, t, $^1J(^{11}B,^1H) = 110$ Hz] and $LiB(S_2C_6H_4)_2$, **17** [12.1, s].

Storing the solution at -30°C provided single crystals of dimeric **17**·2THF, analyzed by X-ray structure determination.

6.14. Lithium dihydrido-1,2-ethanedithiolato borate (15)

In analogy to **14** $LiBH_4$ (220 mg, 10.1 mmol) was treated with ethanedithiol (951 mg, 10.1 mmol) in a total of 60 ml of THF. After 4 h the ^{11}B-NMR spectrum showed the presence of 3 species with one dominating: $LiBH_4$ [$\delta = -41.6$, quint. $^1J(^{11}B,^1H) = 81$ Hz], $LiH_2B(S_2C_2H_4)$ [$\delta = 13.2$, t, $^1J(^{11}B,^1H) = 111$ Hz] and $LiB(S_2C_2H_4)_2$ [$\delta = 11.1$, s]. Ratio = 2:96:2. Reducing the volume of the solution in vacuo to ≈ 20 ml followed by storing at -30°C yielded clear crystals of composition **18**·2THF after 48 h. Yield: 1.32 g, (68%), $\delta^{11}B = 11.0$).

6.15. X-ray structure determinations

Data collection was performed with Mo–K_α radiation employing a graphite monochromator at 193 K on a Siemens P4 diffractometer equipped with a low-temperature device LT2 and a CCD area detector. Crystals

were transferred from the cold mother liquor into precooled perfluoro ether oil. The selected crystal was mounted on the tip of a glass fiber and rapidly put on the goniometer head cooled with a stream of cold nitrogen gas. The dimensions of the unit cells were calculated from the reflections collected on 15 frames each of five different runs and setting angles by changing φ by 0.3° for each frame. Data were collected in the hemisphere mode of the program SMART [38] with 10s/frame exposure time. Two different χ settings were used and φ changed by 0.3° per frame. Data on a total of 1290 frames were reduced with the program SAINT [39], and the structures solved by direct methods implemented in the program SHELXTL [40]. Non hydrogen atoms were refined anisotropically, hydrogen atoms bound to carbon atoms were place in calculated positions and refined as riding on its C atom. Hydrogen atoms bonded to the boron atoms were found in the difference Fourier synthesis. They were freely refined, in the final cycles with fixed isotropic isotropic thermal parameters. Table 3 contains relevant selected data for cristallography, data collection and structure refinement.

7. Supplementary material

Crystallographic data have been deposited with the Cambridge Crystallographic Data Centre, specifiying the authors, the literature citation, and the CCDC nos.: 143756 (**2**), 143757 (**9**), 143578 (6a THF TMEDA), 143759 (**4** PMDTA), 143760 (**10** THF TMEDA), 143761 (**17** 2THF), and 148402 (**6a** 2THF). Further information may be obtained from The Director, Cambridge Crystallographic Data Center, 12 Union Road, Cambridge CB2 1EZ, UK (Fax +44-1223-336033; e-mail: deposit@ccdc.cam.ac.uk or www: http://www.ccdc.cam.ac.uk).

Acknowledgements

We thank Fonds der Chemische Industrie and Chemetall GmbH for generous support, P. Mayer for the recording of many NMR spectra, and E. Kiesewetter for recording IR spectra.

References

[1] Paper 25 of this series: H. Nöth, G.E.W.J. Wagner, Z. Naturforsch. Teil B 54 (1999) 993.
[2] H.-H. Giese, H. Nöth, W. Ponikwar, St. Thomas, M. Warchhold, Inorg. Chem. 38 (1999) 4188.
[3] H.-H. Giese, H. Nöth, St. Thomas, Eur. J. Inorg. Chem. (1998) 941.
[4] A. Heine, D. Stalke, J. Organomet. Chem. 542 (1997) 25.
[5] D.R. Armstrong, W. Clegg, H.M. Colquhoun, J.A. Daniels, R.E. Mulvey, I.R. Stephenson, K. Wade, J. Chem. Soc. Chem. Commun. (1987) 630.
[6] D.L. Reger, J.E. Collins, M.A. Mathews, A.L. Rheingold, L.M. Liable-Sands, I.A. Guzei, Inorg. Chem. 36 (1997) 6266.
[7] A.S. Antyshkina, G.G. Sadikov, M.A. Porai-Koshits, V.N. Konoplev, A.S. Siozareva, T.A. Silina, Koord. Khim. 19 (1993) 596.
[8] (a) N.A. Bell, H.M.M. Shearer, C.B. Spencer, J. Chem. Soc. Chem. Commun. (1980) 711. (b) Acta Cryst. Sect. C 39 (1983) 694.
[9] The only structure so far reported is for $Li(H_2Bmes_2)\cdot(DME)_2$. J. Hooz, S. Akiyama, F.J. Cedar, M.J. Bennet, R.M. Triggle, J. Am. Chem. Soc. 96 (1974) 274.
[10] H. Nöth, S. Thomas, M. Schmidt, Chem. Ber. 139 (1996) 451.
[11] B.F. Spielvogel, F.I. Ahmed, M.K. Das, A.T. McPhail, Inorg. Chem. 23 (1984) 3263.
[12] D.J. Saturnoi, M. Yamauchi, W.R. Clayton, R.W. Nelson, S.G. Shore, J. Am. Chem. Soc. 97 (1975) 6063.
[13] R. Köster, G. Seidel, Inorg. Synth. 22 (1983) 198.
[14] H.C. Brown, B. Singaram, P.C. Mathew, J. Org. Chem. 46 (1981) 2712.
[15] H.C. Brown, B. Singaram, P.C. Mathew, J. Org. Chem. 46 (1981) 4541.
[16] H.C. Brown, M.V. Ragaishveri, U.S. Racherla, J. Org. Chem. 52 (1987) 728.
[17] W. Biffar, H. Nöth, D. Sedlak, Organometallics 2 (1983) 579.
[18] B. Singaram, T.E. Cole, H.C. Brown, Organometallics 3 (1984) 1520.
[19] G.T. Jordan, F.-C. Liu, S.G. Shore, Inorg. Chem. 36 (1997) 5597.
[20] J. Knizek, Diploma Thesis, University of Munich, 1996.
[21] (a) D. Männig, Doctoral Thesis, University of Munich, 1985. (b) D. Männig, H. Nöth, J. Chem. Soc. Dalton Trans. (1985) 1689.
[22] G.T. Jordan, IV, S.G. Shore, Inorg. Chem. 35 (1996) 1089.
[23] M. Bremer, Doctoral Thesis, University of Munich, 1996.
[24] H. Siebert, Anwendungen der Schwingungsspektroskopie in der anorganischen Chemie, Springer, Berlin, New York, 1966.
[25] W.J. Grigsby, P.P. Power, J. Am. Chem. Soc. 118 (1996) 7981.
[26] X. He, J.F. Hartwig, J. Am. Chem. Soc. 118 (1996) 1696.
[27] R.E.v. Spence, W.E. Piers, Y. Sun, M. Parvez, L.R. McGillrary, M.J. Zavorotko, Organometallics 17 (1998) 2459.
[28] J. Liu, E.A. Meyers, S.G. Shore, Inorg. Chem. 37 (1998) 496.
[29] GAUSSIAN-98, Revision A.5, M.J. Frisch, G.W. Trucks, H.B. Schlegel, G.E. Scuseria, M.A. Robb, J.R. Cheeseman, V.G. Zakrzewski, J.A. Montgomery, Jr., R.E. Stratmann, J.C. Burant, S. Dapprich, J.M. Millam, A.D. Daniels, K.N. Kudin, M.C. Strain, O. Farkas, J. Tomasi, V. Barone, M. Cossi, R. Cammi, B. Mennucci, C. Pomelli, C. Adamo, S. Clifford, J. Ochterski, G.A. Petersson, P.Y. Ayala, Q. Cui, K. Morokuma, D.K. Malick, A.D. Rabuck, K. Raghavachari, J.B. Foresman, J. Cioslowski, J.V. Ortiz, B.B. Stefanov, G. Liu, A. Liashenko, P. Piskorz, I. Komaromi, R. Gomperts, R.L. Martin, D.J. Fox, T. Keith, M.A. Al-Laham, C.Y. Peng, A. Nanayakkara, C. Gonzalez, M. Challacombe, P.M.W. Gill, B. Johnson, W. Chen, M.W. Wong, J.L. Andres, C. Gonzalez, M. Head-Gordon, E.S. Replogle, and J.A. Pople, Gaussian, Inc., Pittsburgh PA, 1998.
[30] D. Reger, J.E. Collins, M.A. Methers, A.L. Rheingold, L.M. Liable-Sands, I.A. Gu, Inorg. Chem. 36 (1997) 6266.
[31] N. Edelstein, Inorg. Chem. 20 (1981) 297.
[32] Made from $SnMe_4$ and BBr_3 by a procedure developed in this laboratory.
[33] M.J.S. Dewer, R. Dietz, J. Am. Chem. Soc. 88 (1966) 1344.

[34] R. Köster, G. Seidel, Inorg. Synth. 22 (1983) 198.
[35] B. Singaram, T.E. Cole, H.C. Brown, Organometallics 3 (1984) 1520.
[36] H. Sachdev, Doctoral Thesis, University of Munich, 1995.
[37] C.K. Narula, H. Nöth, J. Organomet. Chem. 287 (1985) 131.
[38] SMART, Siemens Analytical Instruments, V 4.1, 1996.
[39] SAINT, Siemens Analytical Instruments, V 4.1, 1997.
[40] SHELXTL and SHELXTLPLUS, Siemens Analytical Instruments, S.G. Sheldrick, Göttingen, Germany.